IEEE Access
Multidisciplinary ⋮ Rapid Review ⋮ Open Access Journal

Received November 25, 2020, accepted December 4, 2020, date of publication December 21, 2020,
date of current version December 31, 2020.

*Digital Object Identifier 10.1109/ACCESS.2020.3045929*

# Interference Mitigation Through User Association and Receiver Field of View Optimization in a Multi-User Indoor Hybrid RF/VLC Illuminance-Constrained Network

**IMAN ABDALLA[1], (Member, IEEE), MICHAEL B. RAHAIM[2], (Member, IEEE), AND THOMAS D. C. LITTLE[1], (Senior Member, IEEE)**
[1]Electrical and Computer Engineering Department, Boston University, Boston, MA 02215, USA
[2]Engineering Department, University of Massachusetts Boston, Boston, MA 02125, USA

Corresponding author: Iman Abdalla (imanha@bu.edu)

This work was supported by NSF under Grant CNS-1617924.

**ABSTRACT** In this paper we address interference mitigation through user association and receiver field of view (FOV) optimization in a multi-user indoor optical wireless communication (OWC) scenario. We explore several dynamic FOV receiver solutions including steerable (SDFOV) and non-steerable (DFOV) to optimize performance for multiple devices experiencing orientation dynamics. We compare their performance to a baseline fixed FOV receiver (FFOV). Through modeling and simulation we find that SDFOV receivers outperform DFOV by up to 2.6x and FFOV by up to 5.6x in terms of average minimum throughput gain using our test scenario. Similarly, DFOV receivers can achieve up to 2.2x gain over FFOV receivers. For multi-user environments, we compare the performance of coordinated versus distributed system control. Results show that in the worst case, the distributed greedy system performs on average 46%, 16%, and 57% below the coordinated system for SDFOV, DFOV, and FFOV, respectively at a reduced computational complexity compared to the centralized system. We also note that the performance gap in each system diminishes with increasing transmitter Lambertian order. This analysis is done under different room coverage achieved through optimizing the transmitted power to jointly maximize the minimum received power and the standard illuminance range probability at the working plane. Next, we show the impact of self- and random-human blockage at different Lambertian orders on the minimum and average user throughput values. Lastly, we show the gains from employing the hybrid RF/VLC network compared to a VLC-only mode for two different strategies: (1) minimum-throughput-enhancing and (2) sum-throughput-enhancing.

**INDEX TERMS** Visible light communications (VLC), LiFi, dense networks, optical wireless communications (OWC), hybrid RF/VLC, dynamic field of view (FOV), multi-user, interference, self-blockage, user association, random orientation, FOV optimization, resource allocation, load balancing, user association, emission pattern, smart lighting.

## I. INTRODUCTION

The increasingly crowded Radio Frequency (RF) spectrum has motivated researchers to explore ways to opportunistically employ other bands of the electromagnetic spectrum such as mmWave, optical, and THz bands [1]–[3].

In this work we focus on using the visible light range for indoor communications, i.e., visible light communications (VLC) [4], [5] as a complementary technology to RF. Conveniently, these bands do not interfere with each other. Light has the added advantage of ''dual use,'' providing illumination (lighting) while supporting communications. Lighting is ubiquitous, supported by inexpensive infrastructure, and constrained within opaque walls, providing privacy. A great deal of research describes the advantages of the coexistence of both VLC and RF technologies (e.g., [6]–[8]). However, when designing an indoor VLC system, lighting constraints must be considered. One of which is the standard illuminance

The associate editor coordinating the review of this manuscript and approving it for publication was Ding Xu.

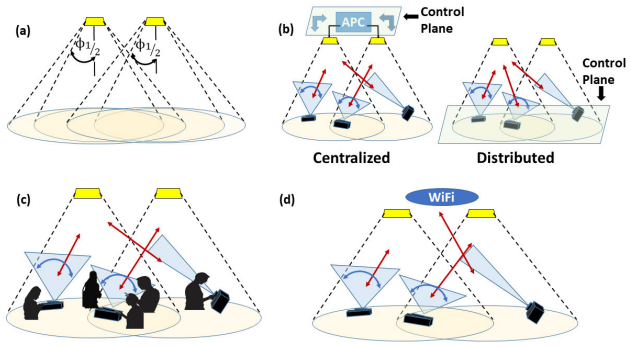


**FIGURE 1.** Sequence of system analysis. (a) Deployment optimization for VLC coverage and illumination; (b) User association and FOV optimization in a multi-user setting under two different system architectures; (c) Evaluation of occlusion effects on the VLC system; (d) Analysis of the hybrid setup of the optimized VLC system and WiFi.

range at the working surface, which is typically $300-500$ lux for an office space [9].

In Cisco's predictions [10], an increase in both the number of devices as well as indoor mobile traffic is forecasted. This supports our study of dense indoor networks. However, with the increase of number of access points (APs), the possibility of interference between cells increases. The AP count growth in the VLC network also begs the question of how to balance the load across APs in the VLC network or, similarly, across tiers in a hybrid RF/VLC network. There exists work, relevant to the interference problem, that focuses on power allocation, user association, load balancing or multiple access techniques [11]–[14]. We discuss interference mitigation in indoor optical wireless networks in [15]. We also study dynamic receiver FOV performance and advantages in prior work [16]–[20] and provide important insights to its usages theoretically and through experimentation.

Based on these two dimensions – the need for balanced illumination, and the need to mitigate interference between users, we set out to (1) optimize luminaire emission and (2) optimize signal quality and user association in a multiple AP setting. We also address how this will be practically managed in either a centralized or distributed way. The conceptional model of this configuration along with the sequence of analysis are illustrated in Fig. 1.

In this model we envision multiple users in a dense hybrid indoor VLC/RF network. Variables and dynamics that affect this system include transmitter parameters: transmitter layout, coverage (emission pattern), illumination, and power. Receiver-side parameters include: receiver orientation, location, FOV, density, and blocking. Finally, system parameters include the management organization: whether via central access point controller (APC) or by distributed and potentially greedy receivers.

Motivated by enhancing user signal quality and user experience in the presence of interference, the novelty of this paper lies in:

- Studying the user association and FOV optimization in a multi-user indoor OWC system under two different FOV receivers; namely, a dynamic FOV (DFOV) receiver and a steerable dynamic FOV (SDFOV) receiver. Then comparing the performance to a baseline fixed FOV receiver (FFOV).
- Comparing the performance of different system architectures in terms of multiple system metrics.
- Comparing the performance of the proposed system under different coverage patterns created through changing the transmitter beam width while maximizing the minimum power received as well as the probability of maintaining illuminance at the standard range.
- Proposing heuristics for the SDFOV receiver as well as proposing a novel orientation based association method for DFOV fairness performance.
- Analyzing the effect of self-blocking as well as randomly located human blockers within the room showing their effect on minimum as well as average user throughput for different Lambertian orders and different system blocking responses (active versus passive).
- Comparing the minimum user throughput as well as the aggregate sum throughput of a dynamic FOV VLC-only system to a hybrid RF/VLC system.

As outcomes of the novel analysis described above, we find the following key results:

- SDFOV outperforms DFOV by up to 2.6x in average minimum throughput gain (5.6x gain over FFOV); DFOV receivers achieve up to 2.2x gain over FFOV receivers in the evaluated configuration.
- The distributed greedy system may reach a lower performance up to 46% less on average (in terms of minimum user throughput) than the coordinated system for SDFOV, 16% for DFOV and 57% for FFOV at a computational complexity reduction from $\mathcal{O}(MN^M)$ to $\mathcal{O}(MN)$.

The remainder of the paper is organized as follows. Section II discusses background work, applications and challenges within our system. Section III defines our system model. Section IV describes our joint optimization of minimum received power and illumination. Section IV discusses the details of our optimization problem. Section V shows our simulation results of the performance metrics. Section VI shows our algorithms and heuristics results for the optimization of the steerable dynamic FOV receiver as well as a heuristic for the DFOV fairness problem. Section VII describes our blockage model and results. Section VIII discusses our hybrid RF/VLC model and its performance results. Section X concludes the paper.

## II. BACKGROUND

Here we discuss prior work, challenges in our novel problem, and broader dynamic FOV applications related to VLC topics impacted by receiver FOV and orientation.

### A. LITERATURE REVIEW

Optimizing the deployment is an essential first step of the network design and is of significant interest to the research

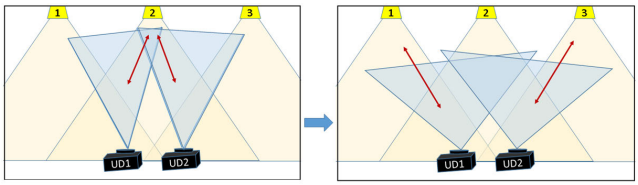


**FIGURE 2.** Importance of FOV optimization and user association.

community. We study different interference cell patterns through changing the emission beam width. This is controlled by the transmitter semi-angle, or the Lambertian order $m$ while assuring a desired illuminance is maintained through a constraint. In [21] the authors vary the transmitter semi-angle to reduce the spatial variations in power. The work in [22], [23] explores optimizing the Lambertian order to maximize the minimum power in a room. However, the works mentioned do not consider an illuminance constraint.

There is a variety of work focused on user association and load balancing in VLC as well as hybrid VLC/RF networks. In [11] the authors use a college admission model in a matching theory to solve a load balancing problem in a hybrid VLC-LTE setup. There is also work focused on power allocation and user association (directing users to access points). In [12] the authors study power allocation and user grouping while employing Non Orthogonal Multiple Access (NOMA) in a multi-cell VLC network. Meanwhile, [13] studies a joint load balancing and power allocation in a hybrid VLC/RF network setup. The authors propose an iterative algorithm to distribute users on the APs and distribute the powers of the APs on their users. In [14], a cooperative load balancing technique is proposed that can achieve higher proportional fairness and area spectral efficiency in comparison with a LiFi only network. In comparison, our work studies the novel problem of joint user allocation and FOV optimization while addressing load balancing in the hybrid RF/VLC model as well as the centralized VLC-only system.

Our prior work is also relevant here. We show: (1) The impact of orientation and FOV on signal reception validated with experimental data [18], [20]. (2) A novel dynamic FOV receiver with performance prediction and experimental validation [16] and its extension to dynamic tracking (steering to point the receiver to the center of a transmitter) [17]. And (3) Resource reuse, coverage perspectives and interference mitigation using dynamic FOV receivers [19]. Interference between indoor users in OWC networks and possible mitigation solutions are reviewed in our prior work in [15]. Here we adopt a channel isolation methodology and study how it can provide gains in the system compared to a wide-FOV non-isolating receiver.

### B. CHALLENGES IN THE NOVEL USER ASSOCIATION AND FOV OPTIMIZATION

The user association and FOV optimization are tightly coupled. We show a simple example of this in Fig. 2 where both users 1 and 2 are located closer to transmitter 2 ($Tx_2$). It may

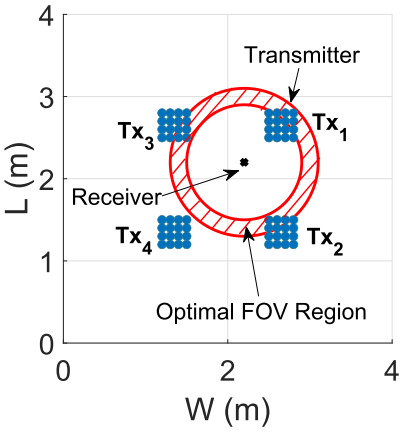


**FIGURE 3.** FOV optimization challenges in a multi-element transmitter configuration.

seem that the association solution would be to have them both connect to $Tx_2$ and share the cell resources or suffer from interference generally. However, if we allow their FOVs to grow so each one can see the more distant transmitter closest to it as in Fig. 2 (right), then User 1 connects to $Tx_1$, User 2 connects to $Tx_3$ and $Tx_2$ is turned off. The result is better individual and system throughput. The problem also depends on the user density; if there were a third receiver that would cause $Tx_2$ to be ON, then it would cause the highest interference on Users 1 and 2 and the best allocation/FOV solution would be different.

Fig. 3 shows the challenge of FOV optimization specifically for the non-steerable dynamic FOV receiver through another example. In this case the receiver is shown centered in a FOV with a flat orientation and connected to $Tx_1$. In case of point-source transmitters, the solution is easier because the optimized FOV will just be the minimum FOV that allows the receiver to see the transmitter. In our configuration, we assume a more practical non-point-source transmitter that we model as consisting of a grid of point-source elements. If the receiver sees all of $Tx_1$, interfering components come into view from both $Tx_2$ and $Tx_3$. To remove interference completely, the FOV must reduce to the smaller illustrated circle. However, this is not necessarily the best solution because of the trade-off between signal strength and interference. This is why the region between these two circles is the optimal FOV region. The optimal FOV is the one that finds the right combination of desired and interfering elements that gives the best signal to interference plus noise ratio (SINR). Other factors that determine the best solution include: which transmitters are actually ON, the receiver location and orientation, user density, and transmitter spacing.

### C. BROADER APPLICATIONS

In this work we focus on employing dynamic FOV receivers to enhance system communication performance in typical indoor illumination scenarios. However, there are other applications in which a dynamic FOV has utility. This includes applications in vehicular communications and light-based

**TABLE 1. Acronyms.**

| Acronym | Description |
|---|---|
| AP | Access Point |
| APC | Access Point Controller |
| CDF | Cumulative Distribution Function |
| DFOV | Dynamic Field of View |
| FOV | Field of View |
| FFOV | Fixed Field of View |
| LED | Light Emitting Diode |
| LOS | Line of Sight |
| MINLP | Mixed-Integer Nonlinear Program |
| PSD | Power Spectral Density |
| PDF | Probability Distribution Function |
| SDFOV | Steerable Dynamic Field of View |
| SINR | Signal to Interference plus Noise Ratio |
| SNR | Signal to Noise Ratio |
| UD | User Device |

positioning. For example, for positioning, a wide FOV is advantageous in finding more light sources to accurately position a device, but also causes increased noise which results in higher root mean square (RMS) error in the localization. This trade-off is described in [24]. In vehicular communications, wide FOV provides wider receiver scope [25] where receiver scope is analogous to transmitter coverage but on the receive side [19]. An enlarged scope has the potential to include more interfering sources. However, a narrow FOV becomes challenged in terms of sustaining alignment between vehicles. Setting a fixed narrow FOV also proves non-beneficial as the optimal FOV will change with the proximity of the transmitter/receiver pair. Steerable DFOV receivers add the advantages of protection of the communication quality under orientation effects and dealing with alignment challenges. This can be very beneficial in relay systems where an SDFOV receiver can be used to relay messages to devices that lack line of sight (LOS) communication.

## III. VLC SYSTEM FRAMEWORK

In this section we describe the details of our standalone VLC system model including, assumptions, receiver specifications, and target performance metrics. Because we care about illuminance, we are particularly interested in average optical power as this is what constrains the transmitted signal. Table 1 provides a summary of the acronyms used in the paper.

### A. CHANNEL MODEL

We assume rectangular-format light sources (transmitters), each consisting of a grid of $w \times l$ point sources (e.g., LED elements).

Fig. 4 shows the hybrid RF/VLC network, the variable receiver location, orientation, FOV, and the parameters involved in our analysis, described later on in this section. We study the LOS optical channel gain. We do not study the effect of reflections as in most environments their effect can be neglected [26]. The element LOS optical channel DC gain [27], the gain from a transmitting element to the receiver, as shown in Fig. 4, is defined as:

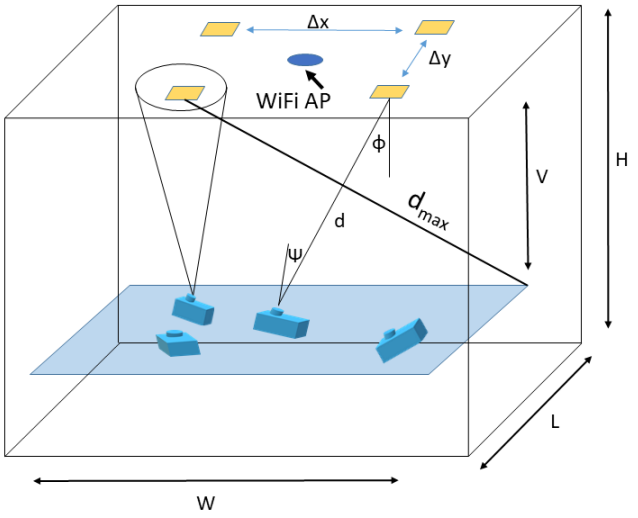


**FIGURE 4. Room layout emphasizing variable device orientation, location, and FOV in a hybrid RF/VLC network.**

$$H^{ji}_{DC,e}(\phi_{ji}, \psi_{ji}, d_{ji}) = \frac{P^{(ji)}_{r,e}}{P^{(ji)}_{t,e}} = \frac{G_T(\phi_{ji})G_R(\psi_{ji})}{d^2_{ji}} \quad (1)$$

where $P^{(ji)}_{t,e}$ and $P^{(ji)}_{r,e}$ are the optical power transmitted and received from the $i$-th element within transmitter $j$, respectively. $\phi_{ji}$ is the emission angle, $\psi_{ji}$ is the acceptance angle, and $d_{ji}$ is the distance between the receiver and the element. Each of the parameters defined with subscript/superscript $ji$ is used to describe the point source element $i$ within source $j$. The subscript $e$ indicates element models. The transmitter gain or radiant intensity (i.e., $G_T$) and the receiver gain (i.e., $G_R$) are defined as:

$$G_T(\phi) = \frac{m+1}{2\pi}\cos^m(\phi)$$

and

$$G_R(\psi) = A\cos(\psi)1\{\psi < \chi\}$$

respectively. We consider a Lambertian emission with order $m$ and model a photodetector with area $A$ and no filter or optical lens. $\chi$ is the receiver's FOV and $1\{.\}$ represents the indicator function.

We consider signal transmission via Intensity Modulation with Direct Detection (IM/DD). Substituting in eq. (1), the optical power received from element $i$ is evaluated as:

$$P^{(ji)}_{r,e} = \frac{P^{(ji)}_{t,e}(m+1)A\cos^m\phi_{ji}cos\psi_{ji}}{2\pi d^2_{ji}}1\{\psi_{ji} < \chi\} \quad (2)$$

where $P^{(ji)}_{t,e} = P^{(j)}_t\alpha_{ji}$. We define $P^{(j)}_t$ as the optical power transmitted from transmitter $j$; therefore, $\sum_i \alpha_{ji} = 1$. In this paper we consider $\alpha_{ji} = \frac{1}{wl}\forall i$ to normalize the transmitter's power over all the elements that it contains.

The transmitter LOS channel gain which sums over all the elements $i$ within the transmitter $j$ is

$$H_{DC}^{(j)} = \sum_{i=1}^{wl} \alpha_{ji} H_{DC,e}^{(ji)} = \frac{P_r^{(j)}}{P_t^{(j)}}$$

where the total received optical power from the $j$-th transmitter is evaluated as

$$P_r^{(j)} = \sum_{i=1}^{wl} P_{r,e}^{(ji)} \tag{3}$$

In a multi-user setup, we define the SINR of user $u$ connected to the $j$th transmitter as:

$$SINR_u^{(j)}(\chi) = \frac{\sigma_j^2}{\sum_{q,q\neq j} \sigma_q^2 + \sigma_a^2} = \frac{(RP_r^{(j)}(\chi))^2}{\sum_{q,q\neq j} (RP_r^{(q)}(\chi))^2 + \sigma_a^2(\chi)} \tag{4}$$

$\sigma_j^2$ is the variance of the desired signal from the associated transmitter $j$, $\sigma_q^2$ is the interfering signal variance and we sum over $q$ depending on the number of interference signals. $\sigma_a^2$ is the noise current variance and $R$ is the receiver responsivity.

In our shot noise dominated system, we model $\sigma_a^2$ as [28]:

$$\sigma_a^2 = \overline{i_q^2} + \overline{i_d^2} \tag{5}$$

where $\overline{i_d^2}$ is the dark current noise and $\overline{i_q^2}$ is the quantum noise. $\overline{i_q^2} = 2qRP_nB_{VLC}$, $q$ is the electron charge, $B_{VLC}$ is the VLC AP bandwidth and $P_n$ is the optical power incident on the photodiode. Meanwhile, $\overline{i_d^2} = 2qI_dB_{VLC}$ where $I_d$ is the dark current.

$$P_n = \sum_j P_{txDC} H_{DC}^{(j)} \tag{6}$$

We define $P_{txDC}$ to describe the transmitted DC power contributing to the noise and is different from the DC signal power. Both $P_n$ and $P_{txDC}$ are defined in the optical domain.

### B. SYSTEM MODEL

**Assumptions:**

1. User devices are assumed to move in a uniformly random fashion throughout the x-y plane at a fixed receiver height (the working plane, highlighted in Fig. 4). We choose to fix the receiver height for simplicity but realize that performance varies with different receiver heights. This is discussed in [19, Fig. 6] where we show that variable height can cause changes to the optimal FOV.
2. Devices are allowed to have variable orientation. The azimuth angle can take a uniformly random angle between (0-360) degrees as well as the elevation which is between (30-150) degrees. We choose these ranges to ensure that the receiver has visibility to at least one transmitter.

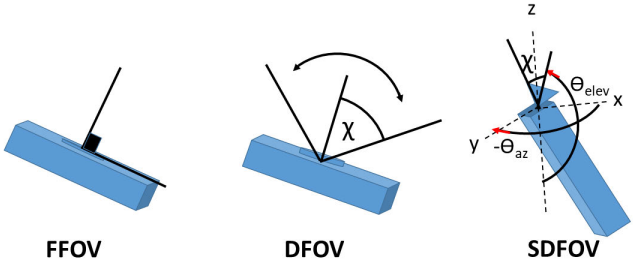


**FIGURE 5.** Receiver structures; Fixed field of view (FFOV), Dynamic field of view (DFOV) and steerable dynamic field of view (SDFOV).

3. Interference is assumed to exist among different APs (inter-cell interference) but for users connected within an AP the resources are divided equally. In terms of individual throughput, assuming no overhead for division of resources, the equation within an AP $j$ for a user $u$ becomes

$$T_u^{(j)} = \frac{B_{VLC}}{2N_{VLC,j}} log(1 + SINR_u^{(j)}) \tag{7}$$

where $B_{VLC}$ is the VLC AP bandwidth and $N_{VLC,j}$ is the number of users connected to VLC AP $j$.[1]

### C. EMPLOYED RECEIVER STRUCTURES

We propose two dynamic field of view receivers and compare their results to the baseline fixed FOV receiver, seen in Fig. 5. We discuss each one next:

#### 1) DYNAMIC FIELD OF VIEW RECEIVER

The DFOV receiver only changes its FOV for the purpose of finding the AP with the best signal [16]. It has no control over its orientation. It can reduce the effect of inter-cell interference by isolating its own desired signal as much as possible. It does not fully guarantee total channel isolation because this depends on the device position as well as its orientation. However, interfering signals may be unavoidable in some scenarios. In terms of hardware complexity, the DFOV receiver is more complex than the baseline fixed FOV receiver but less complex than the SDFOV.

#### 2) STEERABLE DYNAMIC FIELD OF VIEW RECEIVER

The SDFOV receiver [17], has the ability to track a transmitter and change its FOV to get the best signal. Through pointing (steering) analysis it can identify the best elevation and azimuth angles that allow the receiver to attain an acceptance angle $\psi = 0$ with respect to the center of the tracked source. Elevation and azimuth are geometrically deduced as follows:

$$\theta_{elev} = \tan^{-1}\left(\frac{V}{\sqrt{(x_r - x_t)^2 + (y_r - y_t)^2}}\right)$$

$$\theta_{az} = \tan^{-1}\left(\frac{y_t - y_r}{x_t - x_r}\right)$$

[1]The Shannon representation of throughput serves as a tractable model that is not concerned with specific modulation and provides a good approximation of VLC link performance [29], [30]

where $V$ is the vertical distance between the transmitter and the receiver. Then an acquisition analysis provides the optimal FOV (which gives the highest SNR). The optimal FOV can be scanned for but if the receiver knows full information about the transmitter's four corner element locations, as well as its own location, the optimal FOV can also be evaluated as follows:

For this receiver, the optimal FOV is the minimum FOV that allows all elements of the transmitter into the FOV cone without allowing incident interference. This can be evaluated using the formula for dot product as follows:

$$\chi = \cos^{-1}\left(\frac{u_c.u_e}{||u_c||||u_e||}\right)$$

where $u_c$ is the vector from the receiver to the midpoint of the transmitter and $u_e$ is the vector from the receiver to any element within the transmitter. The equation is evaluated for 3D lines so we need to transfer their intersection point to the origin. This can be done by subtracting the receiver location from both known points on the lines. This only needs to be evaluated for the four corner elements. The largest $\chi$ from this calculation is the optimal FOV. The geometry behind this is that due to the random orientation of the receiving element, the FOV cone's intersection with the transmitter plane generally forms an ellipse. By testing the edge elements of the transmitter we find the best intersection of this ellipse (max FOV from the elements) so that all elements are included.

This receiver can achieve full channel isolation as long as the employed transmitters are not touching or overlapping which is a logical assumption. In terms of hardware complexity, it has the highest complexity of the three receivers.

#### 3) FIXED FIELD OF VIEW RECEIVER

The baseline receiver is the FFOV receiver that has its FOV set at $\chi_{FFOV}$. It does not provide channel isolation, however it is the least complex receiver of the three.

### D. PERFORMANCE METRICS

We consider the following performance metrics in evaluating the proposed work.

1. **Fairness:** In the coordinated setting, we solve a max-min problem to get the highest minimum individual throughput. (This takes into account the user throughput after the cell resources have been shared between users within one cell). If this max-min solution can be achieved through multiple user allocations, the one that gives the highest sum is then chosen. This helps the other users not lose performance gains unnecessarily allowing better total system throughput as well. In case of the greedy association, we look at the resultant minimum rate.

2. **Total System Throughput:** The sum of each user throughputs.

3. **Transmitter Utilization Percentage:** The number of active transmitters on average within the system.

4. **Outage Probability:** For a fixed system required throughput, we evaluate the probability that each receiver is unable to meet the requirement. We define an outage as the case when this happens.

## IV. DEPLOYMENT OPTIMIZATION FOR VLC COVERAGE AND ILLUMINATION

In this section we discuss tuning of the Lambertian order and transmit power to vary the transmitter coverage patterns.

For the room shown in Fig. 4, we change the coverage patterns by tuning the transmitter Lambertian order $m$. Controlling $m$ changes the semi-angle of the transmitter ($\phi_{1/2}$) and also changes the inter-cell interference pattern. The trade-off involved is that although having smaller beams creates less interference, the power transmitted has to be reduced to keep the illuminance level in the standard range 300-500 lux [9] at the working plane for an office environment. This is addressed more in depth in [31]. We analyze the effect of changing the coverage pattern on the multi-user scenario when three different receivers are used: the FFOV, DFOV and SDFOV receivers.

Illuminance describes the quantity of luminous flux $\Phi$ falling on a surface [32]. In the illuminance discussion we consider the receiving element (human eye) to have a wide field of view and flat orientation to capture the highest effect of illuminance. This tightly constrains the illuminance. Luminous flux is defined as [33]:

$$\Phi = K_m \int_{380}^{720} P_s V_L(\lambda) PSD(\lambda) d\lambda$$

where $K_m$ is maximum visibility which is about 683 lm/W at $\lambda$ =555 nm [26], $V_L(\lambda)$ is the standard luminosity curve and $PSD(\lambda)$ is the spectral content of the light incident on the receiver. We assume a constant power spectral density (PSD) for the source. $P_s$ in the context of this equation is the radiant power received from all the transmitters, defined as:

$$P_s = \sum_j \sum_i \frac{P_{t,e}^{(ji)}(m+1)\Delta A_s \cos^m(\phi_{ji}) \cos(\psi_{ji})}{2\pi d_{ji}^2} \quad (8)$$

We assume the illuminance is approximately constant over a small enough area. It is then evaluated as luminous flux over this area in which it was observed $\Delta A_s$.

$$I = \frac{\Phi}{\Delta A_s}$$

We consider the area of interest to be the working surface $A_s$ across which illuminance varies. $A_s$ is 0.5 m away from each wall and 72 cm away from the floor level, highlighted and shown in blue in Fig. 4.

In [31] the maximum minimum power received in a space is optimized subject to an illuminance constraint. The minimum power is received from the furthest transmitter away from the edge of the working surface at $d_{max}$, as shown in Fig. 4. However, in our design in eq. (9), we focus on jointly optimizing a weighted sum of the minimum power received and the probability that illuminance lies between the standard ranges, $P_{ill} = P(300 < I < 500)$. $I$ is the illuminance random variable which depends on the receiving element

location $(x_e, y_e)$. Both $x_e$ and $y_e$ are random variables uniform over the working space.

Continuing this analysis, we choose equal weights $w_1 = w_2$. In this way illuminance will not only be constrained (such that the solution will reside at the threshold) but also maximized to provide better user viewing experience. Our system does not assume a dynamically changing Lambertian order hence for each $m$ we aim at giving the users the best illuminance ranges as well as max-min power received. We also simulate results for only maximizing the minimum power received ($w_2 = 0$) and note that the results do not significantly change. Assuming $d_{ji} = d_{max} \forall i$ for the furthest AP $j$, recalling that $P_{t,e}^{(ji)} = \frac{P_t^{(j)}}{wl}$ and looking at the relevant terms containing the optimization variables, the optimization problem becomes:

$$\begin{aligned} &\max_{P_{t,e}^{(ji)},m} \; w_1 \sum_{i}^{wl} \frac{P_{t,e}^{(ji)}(m+1)V^m}{d_{ji}^m} + w_2 P_{ill} \\ &\approx \max_{P_t^{(j)},m} \; w_1 \frac{P_t^{(j)}(m+1)V^m}{d_{max}^m} + w_2 P_{ill} \\ &\quad \text{s.t. } P_{ill} \geq \gamma \\ &\qquad 0 \leq P_t^{(j)} \leq P_{max} \\ &\qquad m > 0 \end{aligned} \tag{9}$$

$\gamma$ in this case is the least allowed standard illuminance probability. The first constraint ($P(300 < I < 500) \geq \gamma$) is to guarantee that the illuminance cumulative distribution function (CDF) mass between 300 and 500 lux has a probability $\gamma$ of the total CDF mass.

## V. USER ASSOCIATION AND FOV OPTIMIZATION

Here we investigate the problem of allocating users to transmitters to yield the best fairness and system sum throughput. The solution and the optimization problem differ based on the receiver used.

For each receiver, we show two possible optimization methodologies, solving it jointly and through decoupling. The results are rendered through Monte Carlo simulations; however, we provide heuristics and show their performance and discuss the limitations of each methodology. The general joint allocation/FOV optimization formulation, for $M$ receivers and $N$ VLC APs, to maximize fairness in this model can be expressed as:

$$\begin{aligned} &\max_{\substack{x_{uj},\chi_u^{(j)},\\ j=1,\ldots,N,\\ u=1,\ldots,M}} \; \min_u \; \sum_{j=1}^{N} \frac{B_{VLC} x_{uj}}{\sum_{k=1}^{M} x_{kj}} \log(1 + SINR_u^{(j)}(\chi_u^{(j)})) \\ &\quad \text{s.t. } x_{uj} \in \{0,1\} \quad \forall u, j \\ &\qquad \sum_{j=1}^{N} x_{uj} = 1 \quad \forall u \\ &\qquad \chi_u^{(j)} \in \mathcal{F} \quad \forall u, j \end{aligned} \tag{10}$$

where $SINR_u^{(j)}(\chi_u^{(j)})$ and $\chi_u^{(j)}$ are the SINR (from eq. (4)) and the FOV of user $u$ connected to transmitter $j$ respectively. Meanwhile, $x_{uj}$ is a binary connection variable; if transmitter $j$ is connected to user $u$ then $x_{uj} = 1$ otherwise it is 0. The second constraint allows the receiver to connect to only a single AP. The last constraint states that $\chi$ should be between the allowed ranges within FOV set $\mathcal{F} \triangleq [\chi_{min}, \chi_{max}]$. $\chi_{min}$ and $\chi_{max}$ are the smallest and largest FOVs achievable by the receiver respectively. The general problem for maximizing the sum throughput resembles eq. (10) but instead the objective function is:

$$\max_{\substack{x_{uj},\chi_u^{(j)},\\ j=1,\ldots,N,\\ u=1,\ldots,M}} \; \sum_{u=1}^{M} \sum_{j=1}^{N} \frac{B_{VLC} x_{uj}}{\sum_{k=1}^{M} x_{kj}} \log(1 + SINR_u^{(j)}(\chi_u^{(j)})) \tag{11}$$

Each of these objective functions inherently penalizes the connection of multiple users to the same AP to promote a more balanced load. The search space $S$ including both sets of variables is $S \triangleq |\{0,1\}|^{MN} \times |\mathcal{F}|^{MN}$, the first term results from the association problem and the second from the FOV optimization. $|\{0,1\}| = 2$, $\chi$ in contrast is continuous. This leads to $S = 2^{MN}|\mathcal{F}|^{MN}$. When applying the constraints on $x_{uj}$ such that 1 receiver is served by 1 AP at most, the association space reduces to $N^M$. As for the FOV space, for a specific association $\{x_{uj}, \forall j, \forall u\}$, it reduces to $|\mathcal{F}|^M$ since each receiver has a single non-zero FOV associated with a single specific transmitter. This is further reduced to $M|\mathcal{F}|$ because there are no dependencies between different receiver FOVs. We then discretize the FOV by $\Delta_\chi$ to search the continuous space, bringing the overall space (complexity) to $S = N^M M \frac{\chi_{max} - \chi_{min}}{\Delta_\chi}$.

### 1) FFOV ANALYSIS

Because the FOV is fixed, the problem reduces to a nonlinear resource division association among users.

### 2) DFOV ANALYSIS

The user association and FOV optimization are tightly coupled. This is clear within this formulation. From eq. (4), the FOV variable $\chi_u^{(j)}$ is present in both the numerator and the denominator of the SINR term. The interference term adds to the complexity of the problem. Also if the interference terms were neglected the problem in terms of FOV only would still be non-convex. The presence of the association variables $x_{uj}$ cause the problem to be a mixed-integer nonlinear program (MINLP) which is known to not have efficient solving techniques.

Unfortunately, methods such as proposed in [34] do not apply in our formulation as the performance function is non-differentiable with respect to FOV. Moreover, the performance function per a single user depends on the resources of other users. This causes strong coupling in the optimization. Each of these properties leads us to develop a different analysis approach.

**TABLE 2. System overhead.**

| Overhead | Coordinated<br>At the Tx side: | Distributed<br>At the receive side: |
|---|---|---|
| FFOV | Receiver Location Info<br>Receiver Orientation Info | Connecting to<br>highest SINR |
| DFOV | Receiver Location Info<br>Receiver Orientation Info | Scanning FOV for<br>highest SINR |
| SDFOV | Receiver Locations | Steering and scanning<br>for highest SNR |

#### 3) SDFOV ANALYSIS

The problem remains similar to the DFOV analysis in terms of variables. However, due to the presence of the pointing and acquisition capabilities of this receiver the SINR term reduces to the SNR. Therefore decoupling the problem, through solving the association problem then optimizing the FOV, can give close sub-optimal solutions.

### A. COORDINATED SYSTEM

This system assumes the usage of a controller. The controller is assumed to know the location of the receivers. In case of FFOV and DFOV receivers, it needs to know the receiver orientation as well. It is able to send the best elevation and azimuth angles to the SDFOV (if necessary). The receivers however are assumed to be able to tune their FOVs on their own. In turn the controller is able to evaluate the best associations between transmitters and receivers for different FOVs. This shows the best performance that the system can achieve in terms of fairness and sum throughput. However, its computational complexity is $\mathcal{O}(MN^M)$. It is NP-hard and cannot be solved in polynomial time.

### B. DISTRIBUTED SYSTEM

In this system the problem is decoupled. Both the association and FOV optimization problem are done at the receivers. We consider the greedy method where each receiver tries to connect to its best channel. The receiver scans the room for best SINR then, when applicable, it changes its FOV to zoom to the best connection. In case of SDFOV, the receiver searches for best SNR. This is highlighted in Table 2.

## VI. VLC SYSTEM PERFORMANCE RESULTS

We demonstrate the performance of the different systems in terms of the metrics described in Section III-D and the simulation parameters of Table 3. We set the number of transmitters $N$ to 4 as well as the receivers $M$ unless otherwise stated. For the dynamic FOV receivers, $\mathcal{F} = [0, 90]$ and for the FFOV, we set $\chi_{FFOV} = 90°$ to be able to see all transmitters in any room and at any orientation. Results are generated and averaged over 10,000 iterations.

### A. VLC DEPLOYMENT

Our model is general; however, we use a specific operating point for investigating and producing results. We do not believe this diminishes the generality of the model. For our simulation setup (room dimension, symmetric transmitters, transmitter spacing, maximum transmit power, and transmitter count, in Table 3), the optimal $(m, P_t)$ pair is (0.3,3.8 W). To test different room coverage, we evaluate the transmit powers to a set of Lambertian orders that exist within the feasible range of the problem in eq. (9), $m = \{0.01, 0.3, 1, 2, 5, 10, 15, 20\}$. The resultant transmit powers are $P_t^{(j)} = \{4, 3.8, 2.5, 1.8, 1.2, 1, 0.8, 0.77\}$ W.

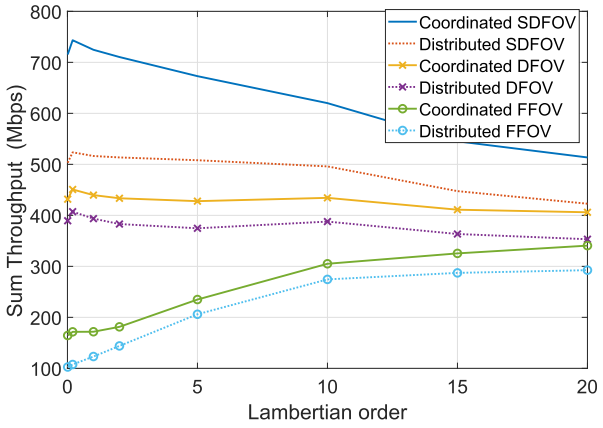


**FIGURE 6. Sum throughput of coordinated vs. distributed for different coverage patterns.**

### B. SYSTEM THROUGHPUT

Fig. 6 compares the average sum throughput of the two systems at different coverage for the three proposed receivers. In the figure, at each point the illuminance CDF mass is centered around 300-500 lux (with the highest possibility that can be reached given this room model and the Lambertian order) by reducing the power for larger Lambertian orders, to allow for best user experience on the working surface in the space. SDFOV has the best performance but it decreases with higher Lambertian order, followed by DFOV which decreases as well. Meanwhile, the FFOV performance is enhanced when the Lambertian order is increased. This is owing to less overlap and less interference. Meanwhile the other two receivers already mitigate interference; thus they are mainly affected by the power drop to maintain illuminance levels.

### C. SYSTEM FAIRNESS

In terms of minimum individual throughput, the receivers still attain their rank in terms of performance as shown in Fig. 7. Notable is that the FFOV receiver does not outperform the greedy association performance of the DFOV receiver. This relationship is maintained as well between the DFOV receiver and the SDFOV receiver. This is due to the FFOV receiver being a strict special case of the DFOV receiver; a lower bound. Likewise the DFOV receiver is a lower bound on the performance of the SDFOV receiver.

Another important result here is that jointly optimizing the Lambertian order for max-min received power and illuminance can enhance the max-min fairness of a system. This optimization result is not normally attained in a multi-user

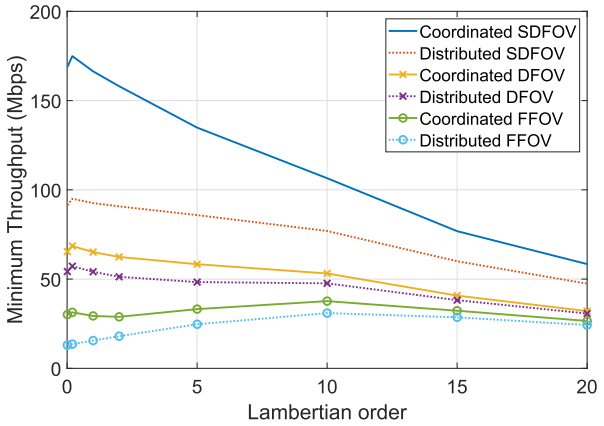


**FIGURE 7.** Fairness of coordinated vs. distributed for different coverage patterns.

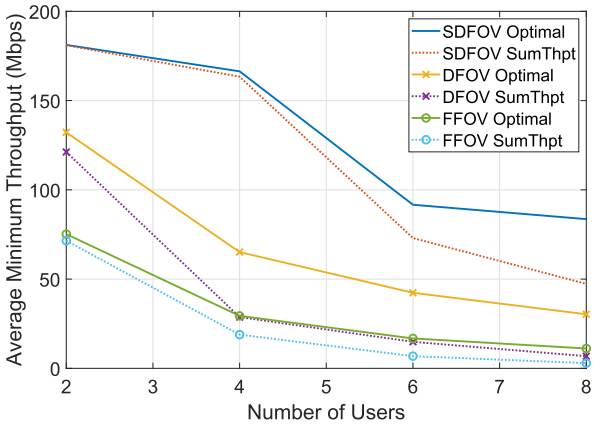


**FIGURE 8.** Fairness of sum throughput optimal mode.

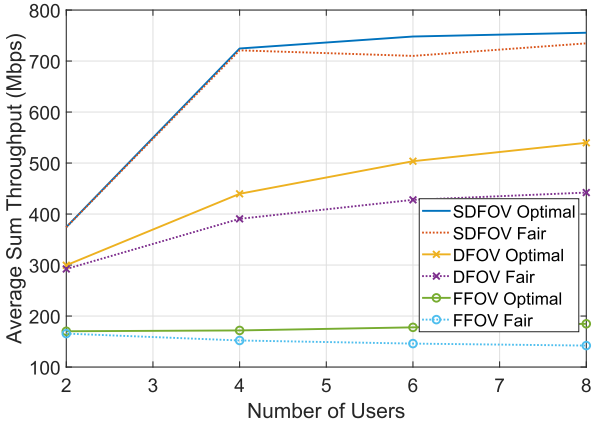


**FIGURE 9.** Sum throughput of fairness optimal mode.

scenario. However when the right receiver is employed, this can change. In this design, the optimal $m$ is 0.3 for highest minimum power received and standard illuminance probability. FFOV receivers do not attain the optimal $m$ simply because the interference effect dominates. In our analysis $m = 10$ gives the best performance for the FFOV minimum rate. However, the SDFOV and DFOV receivers have the ability to mitigate interference much better which enhances their ability to attain best fairness results at the optimal $m$. This is mainly guaranteed for the SDFOV receiver which completely isolates interference.

Analyzing the results, we see that the distributed and coordinated performance for both the FFOV and the DFOV receivers in this setup are closer than their counterpart performance for the SDFOV receiver. The greedy association for the SDFOV receiver substantially fails to meet the coordinated system performance which confirms that the greedy approach does not uncover the full potential of this receiver.

We investigate heuristic approaches to allow the controller to use reduced information about the receivers and still maintain a performance better than the greedy association method in Sections VII-A and VII-B.

### D. FAIRNESS VS. SUM THROUGHPUT TRADEOFF

Here we discuss the effects of targeting fairness on the system sum throughput and vice versa. Fig. 8 shows the system average minimum throughput for a coordinated system that optimizes sum throughput plotted for different number of users. The results for all receivers start to diverge from each other as soon as four users are in the system. However, Fig. 9 shows the system average total throughput of a coordinated system that optimizes fairness as defined in Section III-D. In this figure the curves diverge at a slower rate with the worst case being the DFOV in terms of divergence away from the optimal, but the other two receivers show that maximizing fairness, specially using either SDFOV or FFOV, shows a promising total system throughput as well. Results are plotted for $m = 1$.

### E. TRANSMITTER UTILIZATION PERFORMANCE

Transmitter utilization is an important metric to help understand if the system is balanced and realizing its full potential for multi-user access. The results we show have been averaged over 10, 000 trials that fully covered the room and different device orientation uniformly to provide credible statistical conclusions.

Fig. 10 shows the average transmitter utilization percentage of the sum throughput optimizing coordinated system for different room coverage plotted along with the results of the distributed system. This figure also tells us information about the system load balancing for each receiver employed. The SDFOV receiver utilizes each of the transmitters (one Tx per each Rx) to achieve best sum throughput and also gives best load balancing performance. Second in performance is the DFOV receiver which utilizes almost 90% of the receivers at each Lambertian order. Its inability to steer to a transmitter causes the difference from the SDFOV receiver. As for FFOV utilization, it is highly dependent on the Lambertian order. This is mainly due to the presence of high interference in the lower Lambertian orders that remove its ability to freely choose transmitters. Finally, the distributed system shows similar transmitter utilization percentages for each receiver and each Lambertian order around 68% of transmitters are used on average.

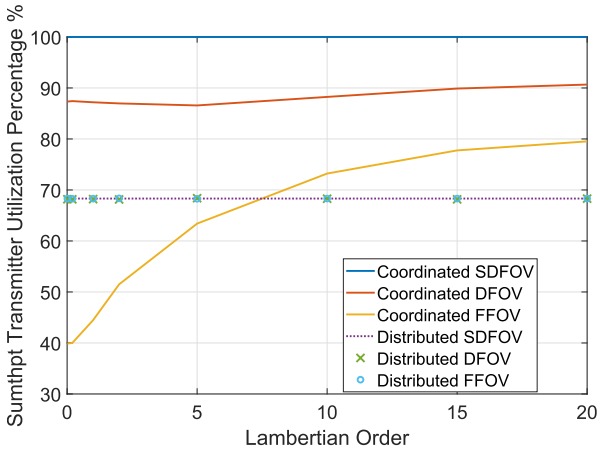


**FIGURE 10.** Transmitter utilization percentage in sum throughput optimal system.

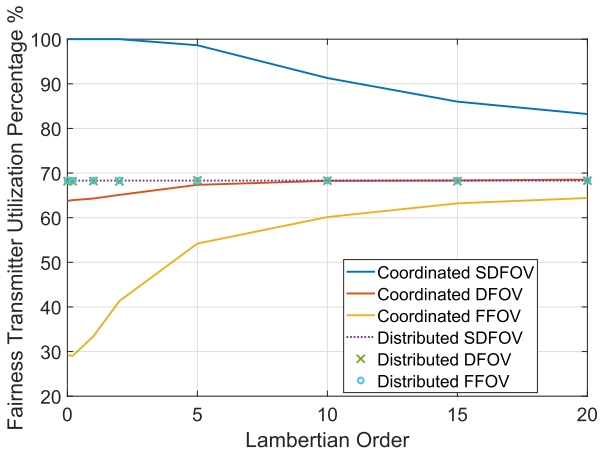


**FIGURE 11.** Transmitter utilization percentage in fairness optimal system.

Fig. 11 shows these statistics for a coordinated system optimizing fairness instead. In this case each of the receivers shows variable performance with different Lambertian orders. The SDFOV receiver is able to achieve best load balancing results at lower Lambertians but with higher ones it gives less flexibility for the minimum throughput user and so load balancing is sacrificed. The same happens to DFOV receivers and the FFOV mostly shows the same performance. Overall the load balancing results are better in the sum throughput optimizing scheme, seen in Fig. 10. This is because the scheme tends to be greedy, by allocating the poorest signal to a transmitter that balances the load instead of a transmitter that helps the minimum throughput user. This does not happen in the max-min allocation and so users may have to share transmitters more often which causes less load balancing.

### F. OUTAGE PROBABILITY

We define an outage as an instance of a user device failing to meet its required throughput. Once a user throughput is less than target throughput $T_{out}$, this user is declared in outage $P_{Outage} = P\{T_u^{(j)} < T_{out}\}$. We set $T_{out}$ to 30 Mbps and

**TABLE 3.** Simulation parameters.

| Parameter | Parameter Description | Value |
|---|---|---|
| Room Size | W×L×H | 4×4×3 $m^3$ |
| $B_{VLC}$ | Bandwidth | $5 \times 10^7$ Hz |
| A | Receiver area | $785 \times 10^{-9}$ $m^2$ |
| $\Delta_x$ | Spacings between Txs in x-axis | 1 m |
| $\Delta_y$ | Spacings between Txs in y-axis | 1 m |
| $P_{max}$ | Maximum Transmitter power | 4 W |
| $w \times l$ | $T_x$ Element grid width × length | $4 \times 4$ |
| $R$ | Responsivity | 28 A/W |
| $V$ | Vertical height bet. Tx and Rx | 1.96 m |
| $\gamma$ | Desired illuminance probability | 0.4 |
| $i_d^2$ | Dark current noise | $68 \times 10^{-20}$ $A^2$ |
| $P_{txDC}$ | Noise DC power | 0.0022 V |
| $No_{WiFi}$ | Noise power spectral density | -174 dBm |
| $P_{WiFi}$ | Transmitted RF power | 27dBm |
| $B_{RF}$ | RF WiFi Bandwidth | 20 MHz |
| $d_h$ | Head diameter men/women | 18/17.5 cm |
| $d_b$ | Body diameter men/women | 41/36 cm |
| $v_l$ | Viewing distance | 36 cm |
| $d_h$ | Head diameter men/women | 18/17.5 cm |
| $l_h$ | Head and neck length men/women | 31.2/29.8cm |
| $l_{bd}$ | Distance between device and body | 20 cm |
| $A_e$ | Office fixed loss factor | 38 dB |
| $B_l$ | Distance dependent loss coefficient | 30 |
| $n$ | Floors/walls between Tx and Rx | 0 |
| $\sigma_g$ | Gaussian standard deviation | 10 dB |

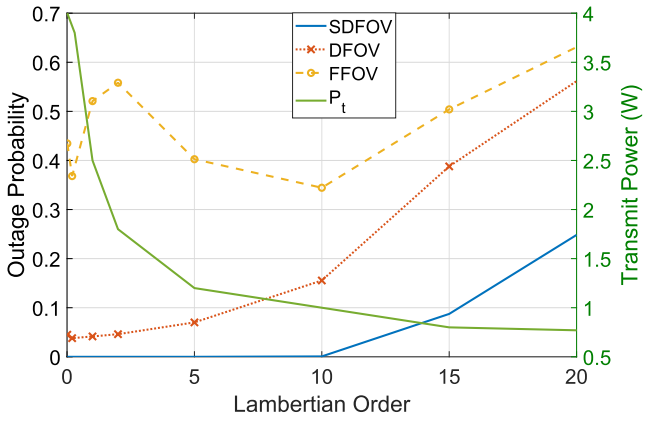


**FIGURE 12.** Outage probability for 4 users at varying lambertian orders.

evaluate how the receivers perform in the fair coordinated system at different Lambertian orders and at a fixed Lambertian order $m = 1$ for different numbers of users. These results are shown in Figs. 12 and 13.

Fig. 12 shows that the SDFOV receiver outperforms the other two receivers but generally deteriorates at large Lambertian orders due to the lower power transmitted for maintaining acceptable illuminance (illustrated on the right-side axis). The DFOV receiver has the lowest outage probability at the optimal $m$ obtained for the system. The FFOV receiver has least performance The FFOV curve begins in a high-interference, high-transmit-power region ($0.01 < m \leq 0.3$) with a low $P_{out}$. It then enters a region of high-interference, low-transmit-power ($0.3 < m \leq 2$) which causes $P_{out}$ to increase. The curve then enters a low-interference, lower-transmit-power region ($2 < m \leq 10$) which shows the lowest $P_{out}$. Finally, the last region ($m > 10$) has the least transmit power coupled with the effect of high Lambertian orders on

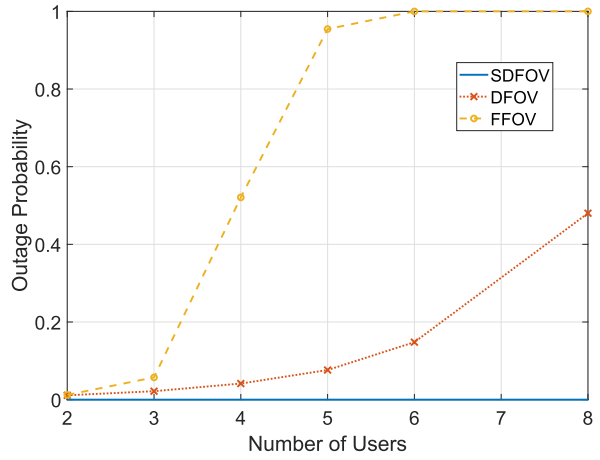


**FIGURE 13.** Outage probability for $m = 1$ and varying number of users.

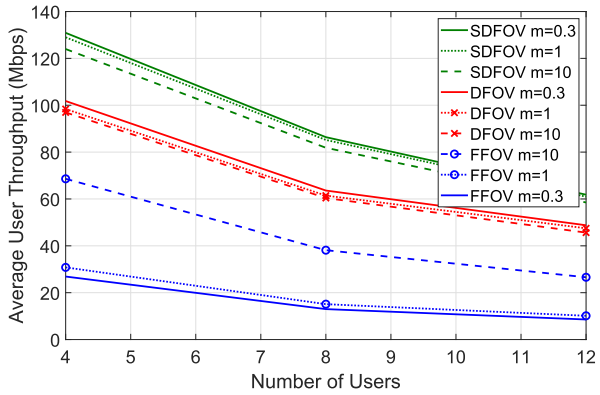


**FIGURE 14.** Distributed system average rate at different Lambertian orders with increased user count.

the channel gain and here $P_{out}$ continues to increase. Fig. 13 shows the outage probability at a fixed Lambertian order $m = 1$ for the range of 2 to 8 users in the system. We notice the same trends and ordering of the receivers with SDFOV outperforming the other two receivers.

In Fig. 14 we show a result related to the distributed system that confirms the relationships between $m$ and average system rate for each receiver. The figure shows the performance of the greedy association for different numbers of users. It also shows the consistency of the performance of each receiver with increasing the number of users in the system. The FFOV receiver shows variable performance with Lambertian orders. In this case better performance with $m = 10$ because of the reduced interference in the system.

### G. ANGLE SENSITIVITY AND PRACTICAL CONSIDERATIONS

In a practical setup it is conceivable that attaining an exact FOV indicated by the optimization might not be possible due to the limits of FOV actuator precision. We tackle this problem for a single user in [17, Fig. 6] showing that inaccurate FOV precision, within less than 2° difference, may cause up to 1.3 dB losses in the signal quality. However, this can be averted as long as the practical FOV is either equal to or slightly larger than the optimal value. In this work though one must take precaution in going too high in FOV increase because this may cause a reduction in performance due to allowing more interfering elements into view.

The dynamic FOV receiver and the steering function have been demonstrated in our testbed in [16] for the purpose of evaluating their performance and demonstrating proof of concept. However, there are other examples of smaller electro-mechanical steering approaches for receiver steering that can be optimized in a practical setting. These include micro-electro-mechanical systems (MEMS) for both transmitters and receivers such as [35], [36].

## VII. ALGORITHM AND HEURISTIC PERFORMANCE

Here we consider heuristic approaches for the optimization problems in eq. (10) and eq. (11) for the SDFOV receiver as well as a fairness heuristic for the DFOV receiver.

### A. SDFOV HEURISTIC APPROACH FOR FAIRNESS

Instead of identifying the exact location of the receiver, the heuristic we propose settles for less information at the controller. We disregard the redundant terms in eq. (2), keeping only the distance between the transmitter and the receiver and the angle of emittance. Both pieces of information are expected to be available on the transmit side without the need for feedback from the receiver (reducing overhead). Then the MINLP problem in eq. (10) becomes decoupled into the binary linear program, defined next in eq. (12), for user association and then FOV optimization can be done at the receiver. Then the controller solves:

$$\begin{aligned} \max_{\substack{x_{uj},\\ j=1,\ldots,N,\\ u=1,\ldots,M}} \quad & \sum_j \sum_u \frac{x_{uj} r_{uj}}{\sum_k r_{kj}} \\ \text{s.t. } & x_{uj} \in \{0,1\} \quad \forall u, j \\ & \sum_j x_{uj} = 1 \quad \forall u \\ & \left\lfloor \frac{M}{N} \right\rfloor \le \sum_u x_{uj} \le \left\lceil \frac{M}{N} \right\rceil \quad \forall j \end{aligned} \tag{12}$$

where $r_{uj} = \log(1 + \frac{\cos^m(\phi_{uj})}{d_{uj}^2})$ is a metric concerning receiver $u$ and AP $j$. The denominator introduces a penalty to reduce the number of receivers connected to the same transmitter. It resembles the sum of number of users from the original problem but it only sums their partial rates if they were connected to the same AP. In this way using the same AP for several users is reduced, load balancing is enhanced and the problem is now linear in the variable $x_{uj}$ instead of the non linear original. This problem encapsulates both the user association among APs as well as system AP load balancing.

The last constraint helps spread the receivers across the transmitters to allow better fairness results and higher minimum throughput per user. This constraint is removed in the case of large Lambertian orders ($m > 5$) because with smaller transmitter semi-angles, it will prove non-beneficial to try

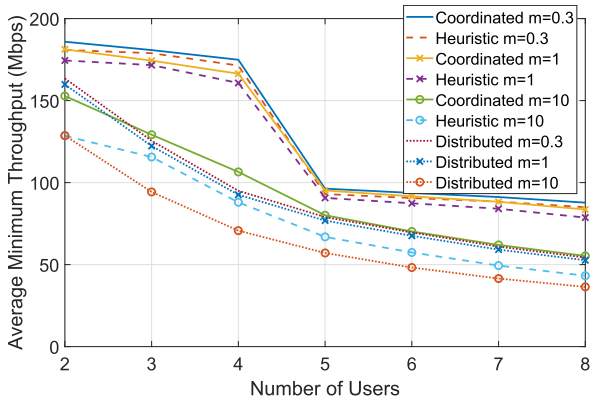


**FIGURE 15.** SDFOV fairness heuristic approach, optimal and distributed solutions.

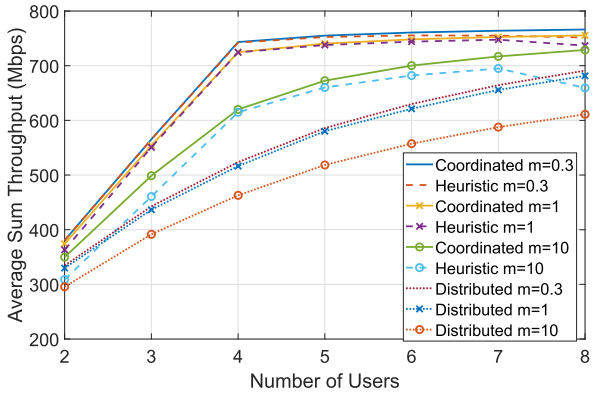


**FIGURE 16.** SDFOV sum throughput heuristic approach, optimal and distributed solutions.

to constrain a certain number of users on the transmitters because there is no longer a guarantee that any transmitter can provide signal everywhere.

We solve this problem using `intlinprog tool` (Copyright 2013-2019 The MathWorks, Inc.). The results for this heuristic show near optimal performance in smaller Lambertian scenarios and more overlap (i.e., higher interference scenarios). Performance for larger Lambertian orders is not as close; however it still outperforms the greedy approach association and in this scenario most system results show better performance at lower Lambertian orders. Fig. 15 shows the average minimum throughput performance of the heuristic and compares it with the coordinated and distributed approaches for each of the proposed receivers. This is performed for three Lambertian orders 0.3, 1, 10 to show the extremes in performance. The heuristic shows near optimal performance in the lower Lambertian orders and starts to diverge when $m = 10$ but it still performs at or above the performance of the distributed method. This figure is plotted for $N = 4$ and $M$ in the range of 2 to 8 receivers.

### B. SDFOV HEURISTIC APPROACH FOR SUMRATE

Here we seek to find the association that leads to best system sum throughput in another attempt to reduce the overhead at the controller. We introduce a weighted binary linear program that only needs the distances between the transmitter and the receiver. The program is defined below:

$$\begin{aligned} &\max_{\substack{x_{uj},\\ j=1,\ldots,N,\\ u=1,\ldots,M}} \sum_u \sum_j x_{uj} w_{uj} r^*_{uj} \\ &\text{s.t. } x_{uj} \in \{0,1\} \quad \forall u, j \\ &\sum_j x_{uj} = 1 \quad \forall u \\ &\left\lfloor \frac{M}{N} \right\rfloor \leq \sum_u x_{uj} \leq \left\lceil \frac{M}{N} \right\rceil \quad \forall j \end{aligned} \tag{13}$$

where $r^*_{uj} = \log(1+\frac{1}{d^2_{uj}})$. $w_{uj} = 1$ for small Lambertian orders and $w_{uj} = \frac{1}{\sum_k r^*_{kj}}$ for $m > 5$.

We also solve this problem using `intlinprog`. The results for this heuristic are very promising as shown in Fig. 16. The data indicate very close performance to the coordinated system at small Lambertian orders. This is due to the fact that the SDFOV receiver is able to eliminate the interference and so the problem reduces to user association according to SNR and FOV optimization without interference. The results degrade with larger Lambertian orders but still outperform the greedy approach. The results plotted are for $N = 4$ and receiver count $M$ between 2 and 8 receivers.

### C. DFOV FAIRNESS HEURISTIC

Here we focus on the fairness problem defined in eq. (10). It has a computational complexity on the order of $O(MN^M)$ which cannot be solved in polynomial time and quickly grows in the number of users and transmitters. The problem is tightly coupled to the variables. Trying to associate the users without adjusting what the receiver sees and vice versa gives sub-optimal solutions.

However, due to the directionality of the optical medium, we can reduce the complexity of the optimal problem to become on the order of $O(M2^M)$ which still grows exponentially but at a slower rate and we also show that with larger number of receivers $M$ the problem grows even closer to the optimal solution. The reason behind this is shown in Fig. 2. The presence of only two receivers in the room gives more free transmitters to choose from and turn 'off' but with the increase in number of receivers, the likelihood that more transmitters are 'on' grows. If (Fig. 2) transmitter 2 is 'on' due to the presence of more receivers, then the receivers UD1 and UD2 would need to connect to transmitter 2 because otherwise it would cause the highest interference on their communications.

#### 1) CLOSEST CHANNEL VS STRONGEST CHANNEL

A combination of system variables triggers the decision of best user-AP association. The receiver location, orientation, transmitter coverage and user density have key roles. In Fig. 17 we show two different definitions, the first channel seen by a receiver FOV as opposed to the stronger channel relative to that receiver. To clarify how we get the best channel in

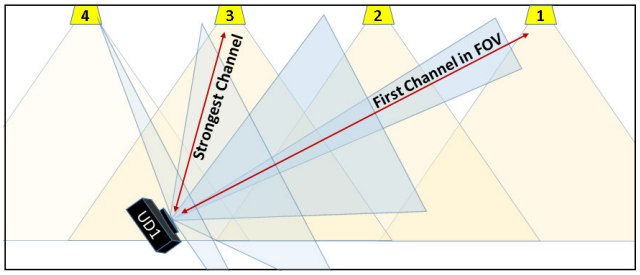


**FIGURE 17.** Difference between strongest channel and first channel in FOV.

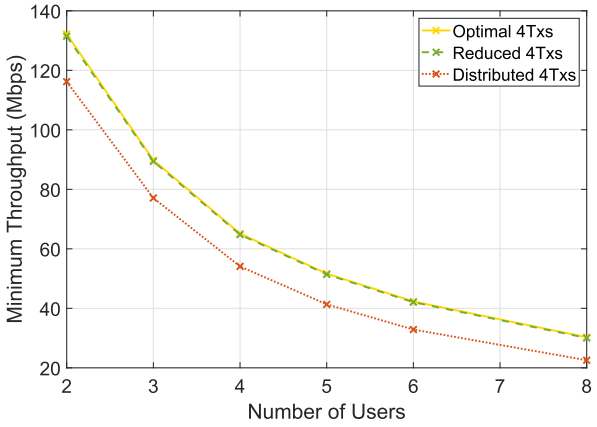


**FIGURE 18.** Performance of reduced complexity in four transmitters scenario.

variable FOV scenarios; the receiver scans different FOVs to get the best channel. If the FOV is fixed at 90° when searching for the best channel then this gives the worst solution on average. This is because this methodology takes away the channel isolation capability and interference isolation. The association based on it is misleading.

The best solution in regards to fairness is not always connecting to the strongest channel. In fact if two receiver were closely located under Tx2 from Fig. 2 then as we showed in the previous example, they are better off connecting to other transmitters.

Through our analysis we have uncovered that for best fairness associations given the system assumptions, the two closest channels (channels with smaller incidence angles) give better performance on average than the two strongest channels (depicted in Fig. 17). This is mainly because the first few channels seen by the FOV give the best possibility of complete isolation from other interferers. Also, narrow FOV allows for higher signal quality and less noise and interference [19]. The other advantage in terms of overhead is that scanning different FOVs for the best channel strength might take longer than only finding the first two transmitters in sight. One should note that, on some occasions the strongest channel is also the first in sight.

We test this observation in a room with four transmitters (Fig. 18). Here we plot the average minimum user throughput with increasing number of users in the optimal coordinated system, the reduced method, and a distributed system that

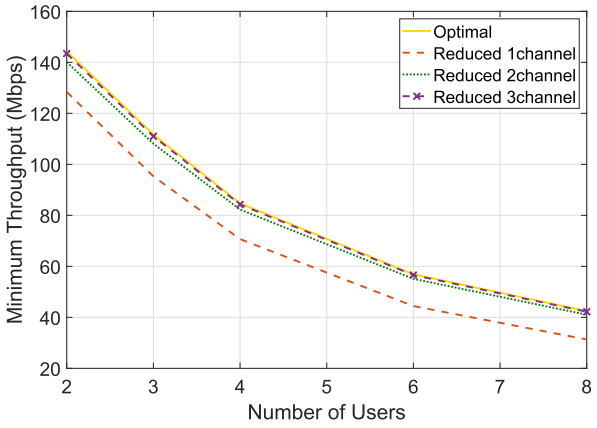


**FIGURE 19.** Performance of reduced complexity in 6 transmitters scenario.

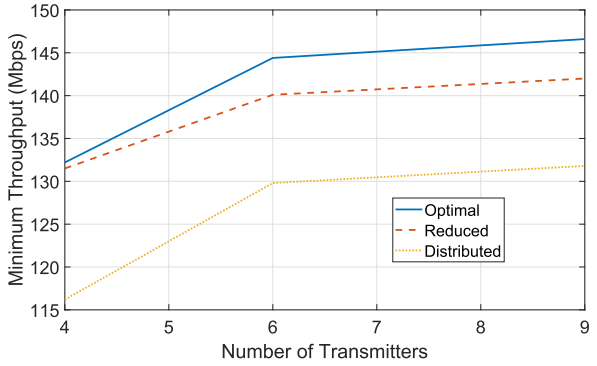


**FIGURE 20.** Reduced complexity performance with growing *n* at worst case two receivers.

picks the best channel. Here the worst accuracy is 99 %. In Fig. 19 we assume 6 transmitters (with the same inter-spacings). In this figure we plot the optimal minimum user throughput along with the reduced method when the first three, two and only one channels are used for association, the worst accuracy is 97% at complexity $\mathcal{O}(M2^M)$ instead of $\mathcal{O}(M6^M)$. It is also worth mentioning that if only one channel information is available then the strongest channel provides marginally better average results than a single close channel.

The worst accuracy is at the lowest number of receivers. The more receivers there are in the room, the better the accuracy. Based on this observation we plotted the worst case of both four and six transmitters along with nine in Fig. 20 to show the accuracy of the worst case compared in growing transmitter number. We did not add more than nine transmitters because we assume 1 m separation in the transmitter grid and any more would be physically impractical. This reduction is even more accurate when transmitters are placed in a line (as opposed to a grid placement). Also, accuracy increases if the separation between the APs is greater than 1 m. We conclude that this analysis approach introduces a novel association method based on device orientation.

## VIII. LINE OF SIGHT BLOCKAGE

We consider the impact of line of sight (LOS) blockage on the performance of the receivers. Channel blockage can be

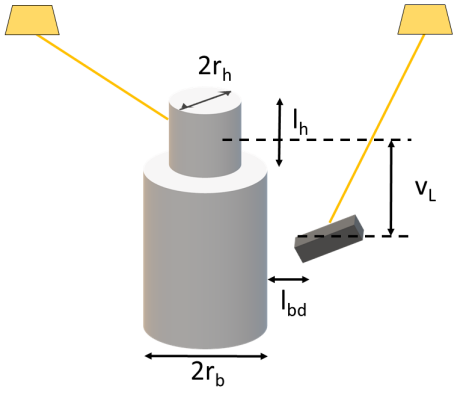


**FIGURE 21.** Approximate human holding smart phone.

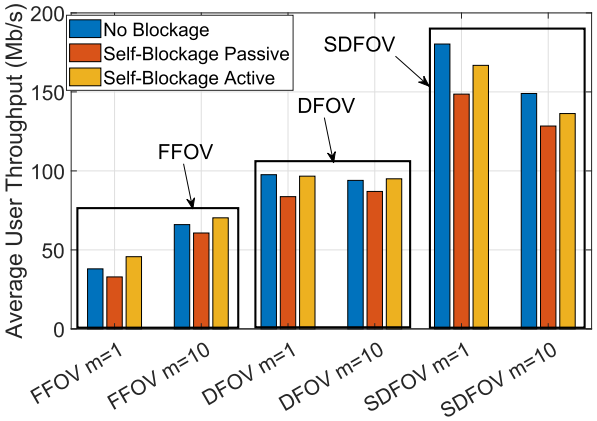


**FIGURE 22.** Average throughput under different blockage systems.

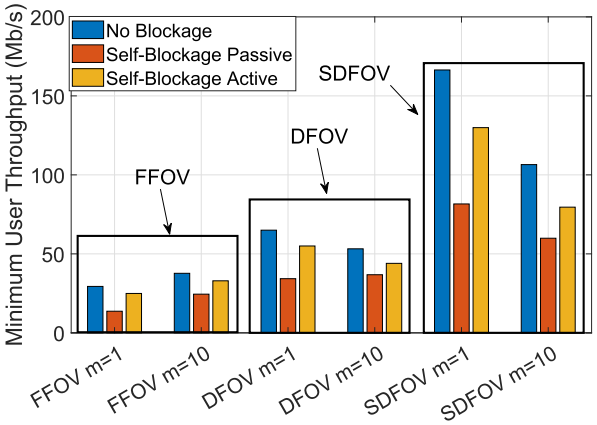


**FIGURE 23.** Minimum throughput under different blockage systems.

characterized through three different factors: occurrence rate, occupation rate, and blockage degree [37]. Occurrence rate defines the presence of channel blockages per unit time. We model this as Poisson arrivals with arrival rate $\lambda_h$. Occupation rate defines the length of time the blockage remains in place. We assume that once the blockage is present it persists throughout the random trial. The unit time is the single random trial time. Finally, the blockage degree is a fraction between 0 and 1 describing how much of the signal gets blocked, with 0 meaning no blockage and 1 meaning full blockage. Most models assume values of 0 or 1 for simplicity. However, due to the fact that we model practical non-point-source transmitters, our model allows partial blockages. This happens when the user or the blockers occlude a fraction of the elements within a transmitter.

The model considers (1) self-blockage and (2) randomly-placed blockers (humans) and assumes that the blockers are seated and using their receiving devices at the working plane. We consider that the difference in geometry for all users sitting or all standing is negligible. However we do not consider a mix between standing and sitting which would require a different model.

As shown in Fig. 21, we model the blocker as a human comprised of two connected cylinders, one representing a head with radius $r_h$ and the other representing a trunk with radius $r_b$. Variables are picked according to the average human head and neck width and length as well as the average human shoulder width respectively. Body size varies according to men and women according to the medical studies/statistics in [38], [39] and we assume a probability of 0.5 for each. The viewing distance between the user and the phone, $v_L$, is adopted from the optometry study in [40]. All parameters are shown in Table 3.

In our analysis, we show both a passive system that gets affected by blockage and has no feedback about its whereabouts, as well as an active system that gets either feedback information from the receivers or is able to detect human presence and associate the users accordingly. Fig. 22 shows the average user throughput performance when no blockage is assumed as well as for self-blockage in both the active and passive systems in a coordinated scheme for all three receiver types and two different emission patterns when four users are in the room. Performance of the minimum user throughput under the same conditions is plotted in Fig. 23.

Figs. 22 and 23 are revealing. First, it is apparent that self-blockage has an effect on throughput performance; however each receiver sees a different degree of impact. The SDFOV is the most affected receiver, and specifically as seen in the the minimum throughput result. The active system helps in enhancing the performance but not as much as in the other receivers. But even in the worst performance case, SDFOV does better, on average, than the other two receiver types. Secondly, the FFOV receiver performs better with a smaller transmitter beam width due to less interference. We also note that in the active system, which is able to correct the associations based on the presence of blockage, the average user throughput from the FFOV receiver is enhanced even compared to the blockage-free case because blockers potentially remove interference sources from their view. Lastly, the DFOV is well balanced, providing throughput enhancements overall.

So far we have demonstrated results of no-blockage versus self-blockage. Figs. 24 and 25 show the effect of self-blockage accompanied by the presence of random human blockers. Their arrival is modeled as Poisson with rate $\lambda_h$. When $\lambda_h = 0$ we revert back to the self-blockage-only

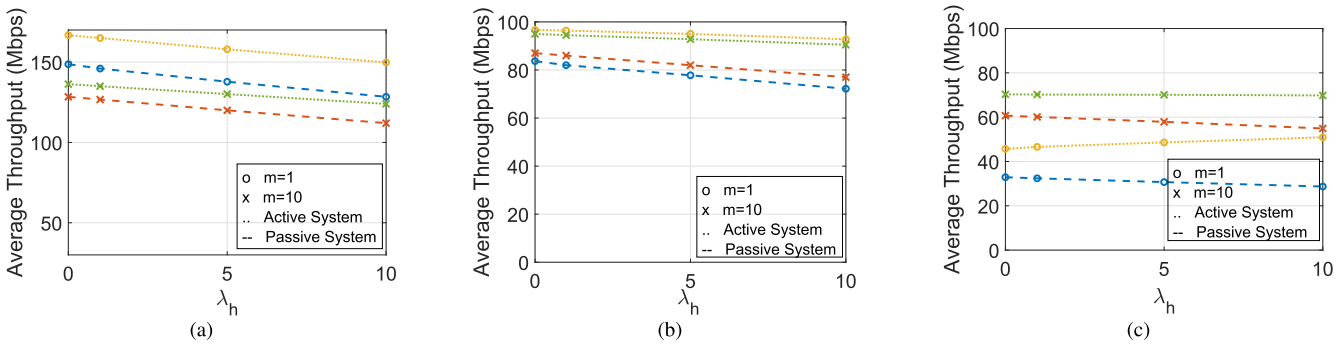


**FIGURE 24.** Active and passive blockage average user throughput performance for all receivers at different $m$ and $\lambda_h$. (a) SDFOV; (b) DFOV; (c) FFOV.

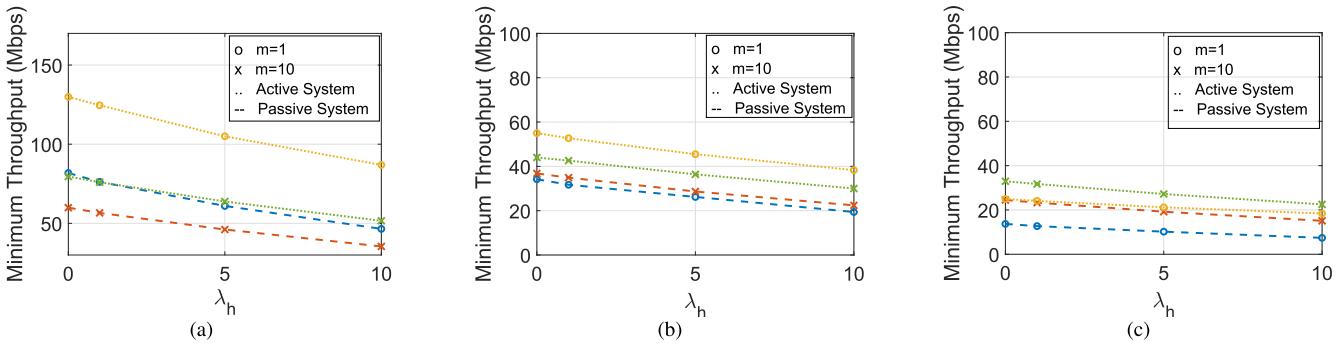


**FIGURE 25.** Active and passive blockage minimum user throughput performance for all receivers at different $m$ and $\lambda_h$. (a) SDFOV; (b) DFOV; (c) FFOV.

case. The results (Fig. 24) show the effect of shadowing on the receiver average throughput for two different Lambertian orders. We also show the effect of active and passive systems here. Fig. 25 shows the effect on minimum throughput.

From Fig. 24 and 25 we observe: (1) The effect blockage has on minimum throughput is more severe. This blockage causes 40-50% reductions in throughput depending on the receiver used. (2) Higher Lambertian orders (smaller beams) show less throughput reduction due to blockages in comparison to the wider-beam case but this is not an indication on the actual performance. (3) DFOV receivers throughout our analysis have better performance with wider beam emissions; however, only in blockage scenarios in the passive systems, the smaller beam emission size $m = 10$ gives marginally better results.

## IX. HYBRID RF/VLC

In this section we combine our performance analysis with the integration of an RF component to yield a hybrid system. The configuration here includes the use of a WiFi AP located at the center of the set of VLC transmitters. Keeping RF congestion in mind, the way we design our system is to try to optimize the user association on the VLC network first then according to a design metric, i.e., fairness or throughput, we start to allocate the users who cannot be accommodated on the VLC to the RF network. Users migrate to RF only if they cannot be supported on any of the VLC APs in the VLC network. The goal in this analysis is to better understand the performance characteristics of such a hybrid model.

### A. RF INDOOR CHANNEL MODEL

We consider a single WiFi AP. The WiFi channel gain at user $u$ is given by:

$$g_u^{WiFi} = |h_u^{WiFi}|^2 10^{\frac{-L(d_u)}{10}}$$

where $h_u^{WiFi}$ is the channel transfer function whose magnitude is Rayleigh distributed. As for the log distance path loss $L(d_u)$, where $d_u$ is the distance between the transmitter and receiver in meters, we follow the JTC (Joint Technical Committee) indoor path loss model which has traits from the Okumura-Hata model [41].

$$L(d_u) = A_e + B_l \log_{10}(d_u) + L_f(n) + X_\sigma$$

where $A_e$ is an environment dependent fixed loss factor in decibels, $B_l$ is the distance dependent loss coefficient, $L_f$ is a floor/wall penetration loss factor in decibels, it can be evaluated using $L_f(n) = 15 + 4(n-1)$ dB where $n$ is the number of floors/walls between the transmitter and the receiver. $X_\sigma$ is a normal (Gaussian) random variable in decibels that has zero mean and standard deviation of $\sigma_g$ (log normal shadowing). The values of the parameters for an office setup are available in Table 3.

The users equally share the single WiFi AP bandwidth $B_{WiFi}$ and so do not interfere with each other. Therefore, the

SNR and the throughput of a WiFi user $u$ respectively are:

$$SNR_u^{WiFi} = \frac{g_u^{WiFi} P_{WiFi}}{B_{WiFi} No_{WiFi}} \quad (14)$$

$$T_u^{WiFi} = \frac{B_{WiFi}}{N_{RF}} log(1 + SNR_u^{WiFi}) \quad (15)$$

where $P_{WiFi}$ is the transmitted WiFi power and $No_{WiFi}$ is the power spectral density of noise at the receiver.

### B. MINIMUM-THROUGHPUT-ENHANCING DESIGN RULE

In this design, we care about the minimum user throughput ($T_{min}$) and so the priority goes to users with outages due to device orientation or location with an ordering from lower to higher user throughput. A user is removed from the VLC network until either there are no more outages or until the minimum rate calculated in the whole network is the highest achieved. Once a user is removed from the VLC network, this frees up bandwidth in a specific VLC AP which in turn helps in alleviating the outage. However, we only give the user the needed rate, the goal is not to give users the highest rates they can achieve. This is to keep the RF free for users that really need it and to not allow excess unnecessary handovers between the two media.

We define the set of users connected to RF and VLC as $\mathcal{WIFI}$ and $\mathcal{VLC}$ respectively. Recall that $N_{RF} = |\mathcal{WIFI}|$ and $N_{VLC,j} = \sum_u x_{uj}$.

The algorithm is shown as Algorithm 1.

**Algorithm 1** Min Throughput ($T_{min}$) Algorithm

1: **Input:** $T_k \triangleq \sum_j x_{kj} T_k^{(j)}$, $\mathcal{VLC} = \{1, 2, \cdots, M\}$, $\mathcal{WIFI} = \emptyset$, $x_{uj} \forall u, j$, $T_{out}$
2: $T_{min}(0) = \min_k T_k$, $u_{min} = \arg\min_k T_k$
3: **for** i=1:M **do**
4: $T_{min}(i) = \min_k T_k$, $u_{min} = \arg\min_k T_k$
5: $\mathcal{WIFI} = \mathcal{WIFI} \cup u_{min}$.
6: $\mathcal{VLC} = \mathcal{VLC} \setminus u_{min}$
7: Recalculate $T_k \forall k \in \mathcal{VLC}$ using eq. (7) and $T_k \forall k \in \mathcal{WIFI}$ using eq. (15). Set $x_{u_{min}j} = 0 \forall j$
8: **if** $T_{min}(i) < T_{min}(i-1)$ **then**
9: Reverse lines (5-6) then Break.
10: **else if** $T_{min}(i) > T_{out}$ **then**
11: Break.
12: **end if**
13: **end for**

Fig. 26 shows the CDF of the minimum individual throughput in case of VLC-only and as well as in the hybrid RF/VLC system at a Lambertian order $m = 1$. A user declares an outage if $T_u^{(j)} < T_{out}$, $T_{out} = 30$ Mbps in this case. At first look, notice that the SDFOV does not experience outage at this $T_{out}$ and thus does not need to use the hybrid mode. This is by design, as long as all users meet their needs there is no need for unnecessary handovers. This behavior alleviates the load on the RF network as well as removes unnecessary latencies. As for the FFOV and the DFOV, if the users can

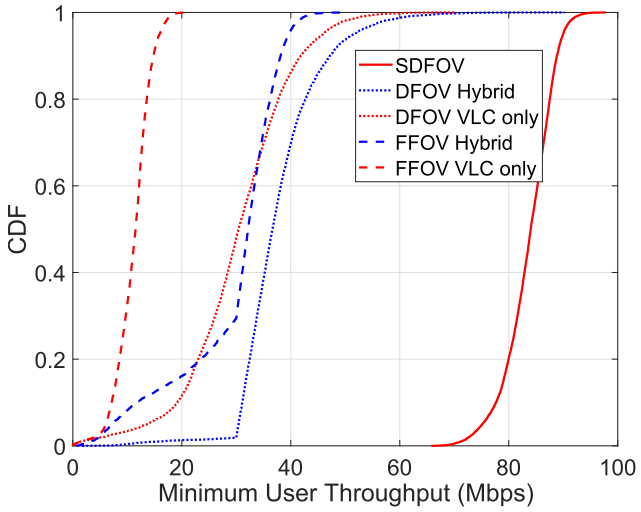


**FIGURE 26.** Minimum user throughput VLC-only vs. hybrid under minimum-throughput-enhancing design at $m = 1$.

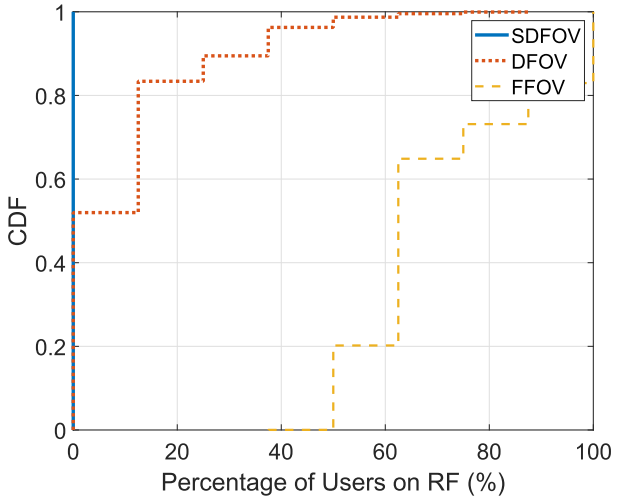


**FIGURE 27.** Percentage of users that transfer to RF when $m = 1$ under minimum-throughput-enhancing design.

tolerate an outage probability of 0.2, then the hybrid network adds a gain of 175% in FFOV case and 41% in case of DFOV.

Meanwhile, Fig. 27 shows the percentage of users that switch to RF. In the case of SDFOV there are none. For DFOV mostly 50% are under 15% of the users in the system (8 users total). Finally the FFOV has the highest percentage of transfers.

Fig. 28 shows the minimum user throughput CDF as well but at $m = 15$ (with a narrower beam). We show the performance of the standalone VLC downlink against the hybrid RF/VLC which is focused on lifting the minimum throughput out of outage. This approach does not allow unnecessary vertical handovers (handover between two media). In this case, SDFOV has outages due to the usage of lower transmission power to attain the illuminance constraint. DFOV performs worse at $m = 15$ than at $m = 1$ which can be seen in the VLC-only result but the hybrid system is able to enhance the performance by 255% on average. As for the

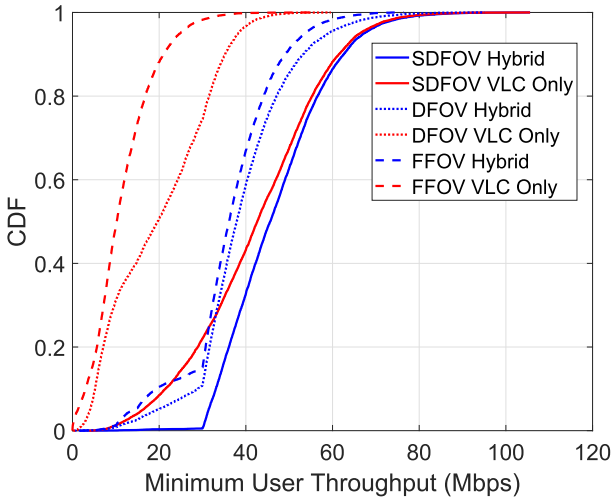


**FIGURE 28.** Minimum user throughput VLC-Only vs. Hybrid under minimum-throughput-enhancing design at $m = 15$.

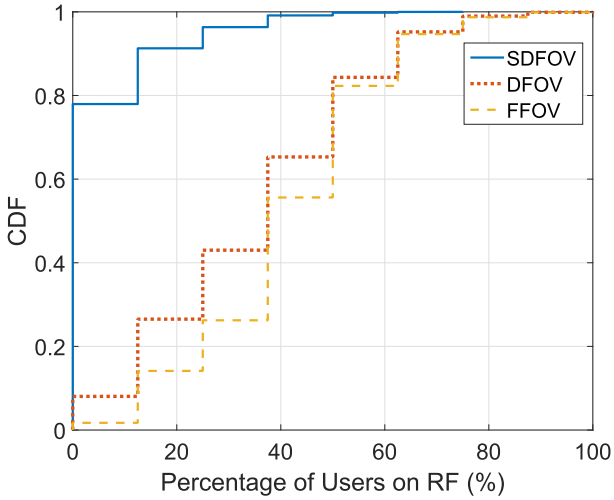


**FIGURE 29.** Percentage of users that transfer to RF when $m = 15$ under minimum-throughput-enhancing design.

FFOV, the individual user throughput has higher ranges in the $m = 15$ case but the minimum throughput is worse; however, its hybrid mode in $m = 15$ is able to achieve better minimum throughput than in the larger emission pattern $m = 1$.

We show the results of transferred user percentage in the $m = 15$ case in Fig. 29. The percentage of transferred users agrees with the overall conclusion that with higher Lambertian order FFOV is enhanced, while the other two receivers perform worse. This is confirmed in Fig. 29 where the percentage of users that transfer to RF when using DFOV and SDFOV increased yet the FFOV percentages decreased.

### C. SUM-THROUGHPUT-ENHANCING DESIGN RULE

In this case we try to enhance throughput and the minimum user rate by moving the weakest users in the VLC network to the RF network until the sum throughput ($T_{sum}$) is maximized. Once the addition of a user reduces the sum throughput, the algorithm stops adding users to the RF. Details are shown in Algorithm 2.

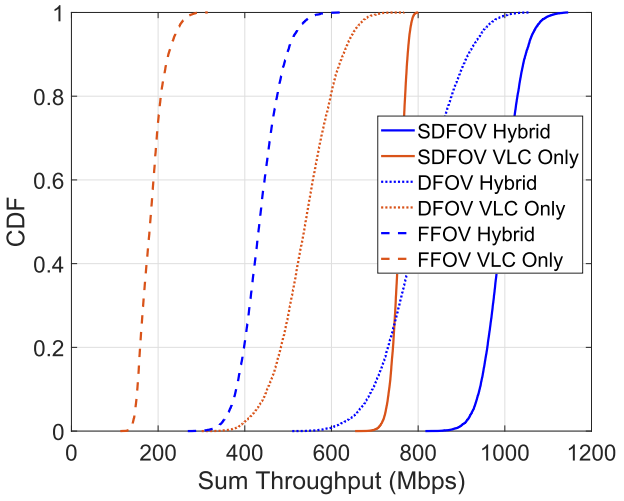


**FIGURE 30.** Aggregate sum throughput VLC-Only vs. Hybrid under sum-throughput-enhancing design at $m = 1$.

**Algorithm 2** Sum Throughput ($T_{sum}$) Algorithm

**Input:** $T_k \triangleq \sum_j x_{kj} T_k^{(j)}$, $\mathcal{VLC} = \{1, 2, \cdots, M\}$, $\mathcal{WIFI} = \emptyset$, $x_{uj} \forall u, j$.
$T_{sum}(0) = \sum_k^{|\mathcal{VLC}|} T_k^{VLC} + \sum_k^{|\mathcal{WIFI}|} T_k^{WiFi}$
**for** i=1:M **do**
  $T_{min}(i) = \min_k T_k$, $u_{min} = \arg\min_k T_k$
  $\mathcal{WIFI} = \mathcal{WIFI} \cup u_{min}$.
  $\mathcal{VLC} = \mathcal{VLC} \setminus u_{min}$
  Recalculate $T_k \forall k \in \mathcal{VLC}$ using eq. (7) and $T_k \forall k \in \mathcal{WIFI}$ using eq. (15). Set $x_{u_{min}j} = 0 \forall j$
  $T_{sum}(i) = \sum_k^{|\mathcal{VLC}|} T_k^{VLC} + \sum_k^{|\mathcal{WIFI}|} T_k^{WiFi}$
  **if** $T_{sum}(i-1) > T_{sum}(i)$ **then**
    Reverse lines(5-6) then Break.
  **end if**
**end for**

Fig. 30 shows the results for the sum-throughput-enhancing RF/VLC system design. It also confirms that the gains from the hybrid RF/VLC system are large in all three receivers. FFOV sees an average sum throughput gain of 136%, DFOV 49% and SDFOV 32%. Meanwhile in Fig. 31 we see that each of the three receivers transfers a high amount of users to the RF AP to achieve such gains. SDFOV transfers up to half the users. DFOV transfers around up to 60% and FFOV up to 90% which in that case leaves one user out of eight on the VLC network. The fact that the dynamic field of view receivers achieve lower hybrid gains than the fixed field of view receiver show that they depend less on the RF network which is ideal for the concept of offloading crowded RF networks.

The drawback of this design lies in allowing a frivolous number of vertical handovers, which can be problematic when more users enter the system. Users who need RF may

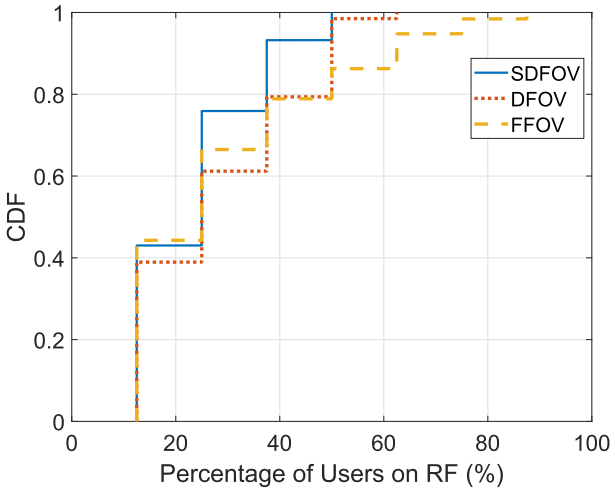


**FIGURE 31.** Percentage of users that migrate to RF under sum-throughput-enhancing design at $m = 1$.

be categorized into (1) fast-moving users (which we do not study here but this is discussed in [16], [42]) because they risk extensive horizontal handovers (handovers that occur within the same medium) along their path; (2) orientation-based outaged users; (3) location-based outaged users; (4) LOS-blocked users; and (5) users in high-density spots which either face high interference from other users or in our case need to share the bandwidth to a degree that affects their service quality.

Lastly, we expect vertical handovers to have higher latency than horizontal ones. In the hybrid design process we argue for making vertical handovers only as needed. Figs. 30 and 31 do not represent the case of minimizing handovers. Fig. 30 shows the huge throughput gains without details. Fig. 31 shows the large percentage of users that migrate to RF to create these high gains.

## X. CONCLUSION

In this work we analyze the problem of joint FOV optimization and user association with load balancing for a multi-user indoor VLC network with the goal of maximizing fairness and system throughput. In our analysis we consider different emission beam widths to understand their impact on system performance. Higher Lambertian orders (smaller beam widths) give lower performance on average. This is mainly due to the need to reduce intensity to maintain the same luminance within the cross-section of the beam. Through the analysis we confirm that for each room design, one might optimize the Lambertian order to enhance illuminance and average fairness in a multi-user scenario if dynamic FOV receivers are used. We also investigate optimization under centralized vs. distributed control. While the centralized (coordinated) system has superior performance, it is more computationally complex and it requires more information from each of the receivers to realize these gains. In contrast, the distributed approach has simplicity and is more readily implemented. Hence, we propose heuristic solutions for the SDFOV receiver that reduce the information required from each receiver. For the DFOV receiver, we show a method to reduce the computational complexity of the optimal solution from $\mathcal{O}(MN^M)$ to $\mathcal{O}(M2^M)$ with 97-99% accuracies in the worst case. We compare the performance of DFOV and SDFOV to the baseline fixed FOV receiver. Simulation results show gains of up to 5.6x of the baseline receiver. We also study how self-blockage and random blockers affect the performance of variable FOV receivers. Results indicate that the variable FOV provides the best overall performance under blockages. Finally, we show how hybrid RF/VLC can provide gains in the max-min user throughput and system throughput through two load balancing algorithms.

## ACKNOWLEDGMENT

Iman Abdalla would like to thank Islam El Bakoury for his valuable input and insight.

## REFERENCES

[1] E. C. Strinati, S. Barbarossa, J. L. Gonzalez-Jimenez, D. Ktenas, N. Cassiau, L. Maret, and C. Dehos, "6G: The next frontier: From holographic messaging to artificial intelligence using subterahertz and visible light communication," *IEEE Veh. Technol. Mag.*, vol. 14, no. 3, pp. 42–50, Sep. 2019.

[2] T. S. Rappaport, G. R. MacCartney, M. K. Samimi, and S. Sun, "Wideband millimeter-wave propagation measurements and channel models for future wireless communication system design," *IEEE Trans. Commun.*, vol. 63, no. 9, pp. 3029–3056, Sep. 2015.

[3] W. Saad, M. Bennis, and M. Chen, "A vision of 6G wireless systems: Applications, trends, technologies, and open research problems," *IEEE Netw.*, vol. 34, no. 3, pp. 134–142, May/Jun. 2020.

[4] P. H. Pathak, X. Feng, P. Hu, and P. Mohapatra, "Visible light communication, networking, and sensing: A survey, potential and challenges," *IEEE Commun. Surveys Tuts.*, vol. 17, no. 4, pp. 2047–2077, Fou. 2015.

[5] H. Haas, "LiFi is a paradigm-shifting 5G technology," *Rev. Phys.*, vol. 3, pp. 26–31, Nov. 2017.

[6] M. Rahaim, I. Abdalla, M. Ayyash, H. Elgala, A. Khreishah, and T. D. C. Little, "Welcome to the crowd: Design decisions for coexisting radio and optical wireless deployments," *IEEE Netw.*, vol. 33, no. 5, pp. 174–182, Jul. 2019.

[7] Z. Li, S. Shao, A. Khreishah, M. Ayyash, I. Abdalla, H. Elgala, M. Rahaim, and T. Little, "Design and implementation of a hybrid RF-VLC system with bandwidth aggregation," in *Proc. 14th Int. Wireless Commun. Mobile Comput. Conf. (IWCMC)*, Jun. 2018, pp. 194–200.

[8] M. Ayyash, H. Elgala, A. Khreishah, V. Jungnickel, T. D. C. Little, S. Shao, M. Rahaim, D. Schulz, J. Hilt, and R. Freund, "Coexistence of WiFi and LiFi toward 5G: Concepts, opportunities, and challenges," *IEEE Commun. Mag.*, vol. 54, no. 2, pp. 64–71, Feb. 2016.

[9] M. S. Rae, *The IESNA Lighting Handbook–Reference and Application, Illuminating Society of North America*. New York, NY, USA: IESNA Publications Department, 2000.

[10] *Cisco Visual Networking Index: Global Mobile Data Traffic Forecast Update, 2017–2022*, Cisco, San Jose, CA, USA, 2019.

[11] L. Li, Y. Zhang, B. Fan, and H. Tian, "Mobility-aware load balancing scheme in hybrid VLC-LTE networks," *IEEE Commun. Lett.*, vol. 20, no. 11, pp. 2276–2279, Nov. 2016.

[12] X. Zhang, Q. Gao, C. Gong, and Z. Xu, "User grouping and power allocation for NOMA visible light communication multi-cell networks," *IEEE Commun. Lett.*, vol. 21, no. 4, pp. 777–780, Apr. 2017.

[13] M. Obeed, A. M. Salhab, S. A. Zummo, and M.-S. Alouini, "Joint optimization of power allocation and load balancing for hybrid VLC/RF networks," *J. Opt. Commun. Netw.*, vol. 10, no. 5, pp. 553–562, May 2018. [Online]. Available: http://jocn.osa.org/abstract.cfm?URI=jocn-10-5-553

[14] X. Li, R. Zhang, and L. Hanzo, "Cooperative load balancing in hybrid visible light communications and WiFi," *IEEE Trans. Commun.*, vol. 63, no. 4, pp. 1319–1329, Apr. 2015.

[15] I. Abdalla, M. B. Rahaim, and T. D. C. Little, "Interference in multi-user optical wireless communications systems," *Philos. Trans. Roy. Soc. A*, vol. 378, no. 2169, 2020, Art. no. 20190190.
[16] I. Abdalla, M. B. Rahaim, and T. D. C. Little, "Dynamic FOV visible light communications receiver for dense optical networks," *IET Commun.*, vol. 13, no. 7, pp. 822–830, Apr. 2019.
[17] I. Abdalla, M. B. Rahaim, and T. D. C. Little, "Dynamic FOV tracking receiver for dense optical wireless networks," in *Proc. IEEE Global Commun. Conf. (GLOBECOM)*, Dec. 2019, pp. 1–6.
[18] T. Little, M. Rahaim, I. Abdalla, E. Lam, R. Mcallister, and A. M. Vegni, "A multi-cell lighting testbed for VLC and VLP," in *Proc. Global LIFI Congr. (GLC)*, Feb. 2018, pp. 1–6.
[19] I. Abdalla, M. B. Rahaim, and T. D. C. Little, "On the importance of dynamic FOV receivers for dense indoor optical wireless networks," in *Proc. IEEE Int. Conf. Commun. (ICC)*, Jun. 2020, pp. 1–6.
[20] I. Abdalla, M. Rahaim, and T. Little, "Impact of receiver FOV and orientation on dense optical networks," in *Proc. IEEE Global Commun. Conf. (GLOBECOM)*, Dec. 2018, pp. 1–6.
[21] R. Raj, S. Jaiswal, and A. Dixit, "Optimization of LED semi-angle in multipath indoor visible light communication links," in *Proc. IEEE Int. Conf. Adv. Netw. Telecommun. Syst. (ANTS)*, Dec. 2019, pp. 1–6.
[22] D. Wu, Z. Ghassemlooy, H. Le Minh, S. Rajbhandari, and M. A. Khalighi, "Optimisation of Lambertian order for indoor non-directed optical wireless communication," in *Proc. 1st IEEE Int. Conf. Commun. China Workshops (ICCC)*, Aug. 2012, pp. 43–48.
[23] D. Wu, Z. Ghassemlooy, W.-D. Zhong, M.-A. Khalighi, H. L. Minh, C. Chen, S. Zvanovec, and A. C. Boucouvalas, "Effect of optimal Lambertian order for cellular indoor optical wireless communication and positioning systems," *Opt. Eng.*, vol. 55, no. 6, pp. 1–8, 2016.
[24] Y. Zhuang, L. Hua, L. Qi, J. Yang, P. Cao, Y. Cao, Y. Wu, J. Thompson, and H. Haas, "A survey of positioning systems using visible LED lights," *IEEE Commun. Surveys Tuts.*, vol. 20, no. 3, pp. 1963–1988, 3rd Quart., 2018.
[25] B. M. Masini, A. Bazzi, and A. Zanella, "Vehicular visible light networks for urban mobile crowd sensing," *Sensors*, vol. 18, no. 4, p. 1177, 2018.
[26] T. Komine and M. Nakagawa, "Fundamental analysis for visible-light communication system using LED lights," *IEEE Trans. Consum. Electron.*, vol. 50, no. 1, pp. 100–107, Feb. 2004.
[27] J. M. Kahn and J. R. Barry, "Wireless infrared communications," *Proc. IEEE*, vol. 85, no. 2, pp. 265–298, Feb. 1997.
[28] R. Ramirez-Iniguez, S. Idrus, and Z. Sun, *Optical Wireless Communications*. New York, NY, USA: Auerbach Publications, 2008.
[29] M. Kashef, M. Ismail, M. Abdallah, K. A. Qaraqe, and E. Serpedin, "Energy efficient resource allocation for mixed RF/VLC heterogeneous wireless networks," *IEEE J. Sel. Areas Commun.*, vol. 34, no. 4, pp. 883–893, Apr. 2016.
[30] W. Guo, S. Wang, and X. Chu, "Capacity expression and power allocation for arbitrary modulation and coding rates," in *Proc. IEEE Wireless Commun. Netw. Conf. (WCNC)*, Apr. 2013, pp. 3294–3299.
[31] I. Abdalla, M. Rahaim, and T. D. C. Little, "Illuminance constrained emission pattern optimization in indoor VLC networks," in *Proc. IEEE GLOBECOM Workshops (GC Wkshps)*, 2020, pp. 1–7.
[32] Zumtobel Lighting GmbH. (Apr. 2018). *The Lighting Handbook*. [Online]. Available: https://www.zumtobel.com/PDB/teaser/EN/lichthandbuch.pdf
[33] M. B. Rahaim, T. Borogovac, and J. B. Carruthers, "Candles: Communication and lighting emulation software," in *Proc. 5th ACM Int. Workshop Wireless Netw. Testbeds, Exp. Eval. Characterization (WiNTECH)*, New York, NY, USA, 2010, pp. 9–14.
[34] F. Zabini, A. Bazzi, B. M. Masini, and R. Verdone, "Optimal performance versus fairness tradeoff for resource allocation in wireless systems," *IEEE Trans. Wireless Commun.*, vol. 16, no. 4, pp. 2587–2600, Apr. 2017.
[35] T. D. C. Little, D. Bishop, J. Morrison, and I. Matthias. (Oct. 2019). *MEMS Devices for Smart Lighting Applications*. [Online]. Available: https://patents.google.com/patent/US10451808B2/
[36] T. D. C. Little and J. C. Chau. (Dec. 2019). *Visible Light Communications Receiver*. [Online]. Available: https://patents.google.com/patent/US10505629B2/
[37] X. Wu and H. Haas, "Access point assignment in hybrid LiFi and WiFi networks in consideration of LiFi channel blockage," in *Proc. IEEE 18th Int. Workshop Signal Process. Adv. Wireless Commun. (SPAWC)*, Jul. 2017, pp. 1–5.
[38] Wikipedia. (2020). *Human Head*. Accessed: Jul. 1, 2019. [Online]. Available: https://en.wikipedia.org/wiki/Human_head
[39] C. D. Fryar, D. Kruszan-Moran, Q. Gu, and C. L. Ogden. (2018). *Mean Body Weight, Weight, Waist Circumference, and Body Mass Index Among Adults: United States, 1999–2000 Through 2015–2016*. Accessed: Jul. 1, 2019. [Online]. Available: https://stacks.cdc.gov/view/cdc/61430
[40] Y. Bababekova, M. Rosenfield, J. E. Hue, and R. R. Huang, "Font size and viewing distance of handheld smart phones," *Optometry Vis. Sci.*, vol. 88, no. 7, pp. 795–797, Jul. 2011.
[41] S. L. Cebula, III, A. Ahmad, J. M. Graham, C. V. Hinds, L. A. Wahsheh, A. T. Williams, and S. J. DeLoatch, "Empirical channel model for 2.4 GHz IEEE 802.11 Wlan," in *Proc. Int. Conf. Wireless Netw. (ICWN)*, 2011, p. 1.
[42] I. Abdalla, M. B. Rahaim, and T. D. C. Little, "Investigation of outage probability and AP placement for mobile users in indoor VLC system design," in *Proc. IEEE Wireless Commun. Netw. Conf. (WCNC)*, Apr. 2019, pp. 1–6.

**IMAN ABDALLA** (Member, IEEE) received the B.S.E.E. degree from Alexandria University, Egypt, in 2010, and the M.S. degree in wireless technologies from Nile University, Egypt, in 2014. She is currently pursuing the Ph.D. degree from the Electrical and Computer Engineering Department, Boston University. Her current research interests include optical wireless communications, 5G, and heterogeneous networks. Throughout 2013, she interned at Intel Corporation in Oregon, USA. She is also a member of the IEEE Communications Society. She received a Best Paper Award from IEEE Globecom 2018, Abu Dhabi, UAE, in the ONS track as well as the TAOS Technical Committee's Award for Best Paper in the ONS Symposium, 2019, Shanghai, China. She also received Boston University's Graduate Teaching Assistant of the year award 2019.

**MICHAEL B. RAHAIM** (Member, IEEE) received the B.S. degree from the Rensselaer Polytechnic Institute, in 2007, and the M.S. and Ph.D. degrees in computer engineering from Boston University, in 2011 and 2015, respectively.

He was a Postdoctoral Researcher with Boston University from 2015 to 2017. Prior to graduate study, he worked as a Software Engineer with the Honeywell's Firelite Alarms Division. He is currently an Assistant Professor with the Engineering Department, University of Massachusetts Boston. His research interests include wireless communications and dynamic/adaptive wireless networks with a specific focus on optical wireless communications, software defined radio (SDR), and testbed development. He is the Co-Founder of the SDR-Boston user group and the annual New England Workshop on SDR (NEWSDR).

**THOMAS D. C. LITTLE** (Senior Member, IEEE) received the B.S. degree in biomedical engineering from RPI, in 1983, and the M.S. degree in electrical engineering and the Ph.D. degree in computer engineering from Syracuse University, in 1989 and 1991, respectively.

He is currently a Professor with the Electrical and Computer Engineering Department, Boston University. His recent efforts address research in pervasive computing using wireless technologies. This includes optical communications, indoor positioning, and applications related to smart spaces, ecology, healthcare, and transportation. He is also a member of the IEEE Computer and Communications Societies, and the Association for Computing Machinery.